Bioactive Materials 6 (2021) 1491–1511

Contents lists available at ScienceDirect

Bioactive Materials

journal homepage: www.sciencedirect.com/journal/bioactive-materials

Bioinspired mineralized collagen scaffolds for bone tissue engineering

Zhengwei Li [a,b], Tianming Du [a], Changshun Ruan [b,**], Xufeng Niu [a,c,d,*]

[a] Key Laboratory for Biomechanics and Mechanobiology of Ministry of Education, School of Biological Science and Medical Engineering, Beihang University, Beijing, 100083, PR China

[b] Research Center for Human Tissue and Organs Degeneration, Institute of Biomedicine and Biotechnology, Shenzhen Institutes of Advanced Technology, Chinese Academy of Sciences, Shenzhen, 518055, PR China

[c] Beijing Advanced Innovation Center for Biomedical Engineering, Beihang University, Beijing, 100083, PR China

[d] Research Institute of Beihang University in Shenzhen, Shenzhen, 518057, PR China

ARTICLE INFO

Keywords:
Collagen
Mineralization
Scaffold
Bone repair
3D printing
Biomechanics

ABSTRACT

Successful regeneration of large segmental bone defects remains a major challenge in clinical orthopedics, thus it is of important significance to fabricate a suitable alternative material to stimulate bone regeneration. Due to their excellent biocompatibility, sufficient mechanical strength, and similar structure and composition of natural bone, the mineralized collagen scaffolds (MCSs) have been increasingly used as bone substitutes via tissue engineering approaches. Herein, we thoroughly summarize the state of the art of MCSs as tissue-engineered scaffolds for acceleration of bone repair, including their fabrication methods, critical factors for osteogenesis regulation, current opportunities and challenges in the future. First, the current fabrication methods for MCSs, mainly including direct mineral composite, in-situ mineralization and 3D printing techniques, have been proposed to improve their biomimetic physical structures in this review. Meanwhile, three aspects of physical (mechanics and morphology), biological (cells and growth factors) and chemical (composition and cross-linking) cues are described as the critical factors for regulating the osteogenic feature of MCSs. Finally, the opportunities and challenges associated with MCSs as bone tissue-engineered scaffolds are also discussed to point out the future directions for building the next generation of MCSs that should be endowed with satisfactorily mimetic structures and appropriately biological characters for bone regeneration.

1. Introduction

Since infancy, bone tissue always plays a significant role in human life. The unique composition and complex structure of bone determine its important functions in human [1,2], mainly including: protective, supporting, motor, storage and hematopoietic function [3–8]. In general, stiffness and toughness conflicts with each other, while bone tissue behaves these two mechanical properties and performs function at the same time. In natural bone, organic substances (such as collagen fibers) provide toughness [9], while inorganic substances (such as apatite) provide stiffness [10]. The combination of organic and inorganic substances allows bone tissue to exhibit high strength and sufficient toughness [11]. In natural bone, inorganic components account for most proportions, which can reach more than 60%, and organic components only account for about 30% [12,13]. Type I collagen (COL, if there is no special instruction, COL refers to type I collagen) is the most important component of organic phase in bone, which is a force-sensitive protein with a diameter of 80–100 nm [14,15]. Monomer of COL is composed of two α1 chains and one α2 chain, which can form fibrils through self-assembly and appear a characteristic 67 nm horizontal stripe pattern that called the D cycle [15,16]. The organic phase in bone is predominantly calcium phosphate-based minerals and the most component of which is hydroxyapatite (HA) [17]. In addition, there are octacalcium phosphate (OCP), tricalcium phosphate (TCP), amorphous calcium phosphate (ACP) and carbonate-substituted HA [18–21]. The mechanical properties of COL and HA as well as bone with different types, refer to the following Fig. 1 [22–32]. Dissimilar treatment processes and methods for material have influence on mechanical

* Corresponding author. School of Biological Science and Medical Engineering, Beihang University, No. 37 Xueyuan Road, Haidian District, Beijing, 100083, PR China.

** Corresponding author. Institute of Biomedicine and Biotechnology, Shenzhen Institutes of Advanced Technology, Chinese Academy of Sciences, No. 1068 Xueyuan Avenue, Nanshan District, Shenzhen, 518055, PR China.

E-mail addresses: cs.ruan@siat.ac.cn (C. Ruan), nxf@buaa.edu.cn (X. Niu).

https://doi.org/10.1016/j.bioactmat.2020.11.004

Received 17 August 2020; Received in revised form 20 October 2020; Accepted 2 November 2020

properties test [33–35], but rules can still be found. From Fig. 1, we can find that pure COL has better performance in shear modulus and breaking strength, while HA performs better in tensile modulus and ultimate tension strength. The cortical bone exhibits good stiffness and toughness that combine the different mechanical properties of COL and HA. Bone in different parts of the human body exhibits excellent mechanical properties. However, there are certain differences in mechanical properties of different parts bone, which is caused by environment and component's proportion [36].

As for why bone has such excellent mechanical properties, scholars have done many researches and found that this phenomenon is related to the special hierarchical structure of bone. With the development of research methods, the understanding of hierarchical structure is also changing. From the initial seven-level stratification [37], to the subsequent nine-level stratification [38], until the twelve-level stratification structure recently proposed [39]. At the beginning, macromolecular substances were regarded as basic units of bone tissue and the hierarchical structure of these substances was not discussed in detail. Until it can characterize the three-dimensional structure of bone on nanoscale, Stevens and Kroger began to study the hierarchical structure of substances. They proved that COL and HA exist as nested, helix-like patterns in bone, and the hierarchical structure was also extended to twelve-level. Although there are certain differences in the way of bone hierarchical structure, mineralized COL fiber is regarded as the most important level. It can be divided into two parts before the level of mineralized COL fibers. The COL and HA are combined to obtain mineralized COL fibers and become the basic component of the next level [40]. The mineralized COL fibers, which formed by the uniform distribution of HA in COL fibers, are an important step in the development of bone tissue from microstructure to macrostructure and have important significance for the mechanical properties of bone. The COL fibers have nucleation sites for apatite crystal particles [41,42], so they can guide the growth of mineral crystals and arrange them along the fiber long axis [43]. This orderly structure is the reason that bones are anisotropic [44].

When dealing with symptoms such as fractures, bone defects, and nonunion, the most common method in clinical procedure is invasive treatment, which uses metal pins, screws, plates or rods to align and stabilize the bone [45,46]. These metal implants have good strength and integrity, but in addition to possible immune rejection, they can also cause stress shielding, rigidity, infection, chronic pain, and other side effects [46–48]. Autologous transplantation can effectively reduce the risks of immune rejection, while the same type of bone is limited in quantity and quality [49]. The composition and structure of these implants are different from natural bone from a bionic perspective. Moreover, it often requires multiple operations, which may lead to increasing risk of donor sites [50]. In view of the shortcomings of above two methods, tissue engineering is therefore proposed to improve clinical therapy techniques. The appropriate scaffold is fabricated by biomaterials and given more functions for replacing autogenous bone [51,52]. The bone repair scaffold needs to simulate natural bone structure and create an environment similar to the extracellular matrix (ECM), which provide good living situation for cells and tissues. It is also necessary to select the materials with good biocompatibility as natural bones. From the original pure biomaterial scaffolds [53,54], composite scaffolds [55–58], to recently proposed scaffolds loaded with specific functional cells and proteins [59–61], their application in bone repair research is more and more in-depth. In addition to ideal biocompatibility, osteoconductivity and osteoinductivity, the bone repair scaffold should also have economic benefits, non-toxic and non-carcinogenic [62–64].

From the composition of bone, COL and HA were selected to fabricate tissue engineering scaffolds, which has great significance for bone repair. Pure COL scaffolds have inferior mechanical properties, so there are some disadvantages when they are directly used as bone repair materials. Pure apatite scaffolds perform better in strength and hardness but are inadequate in toughness. Moreover, the degradation rate of pure apatite scaffolds is not consistent with new bone formation [65,66]. In

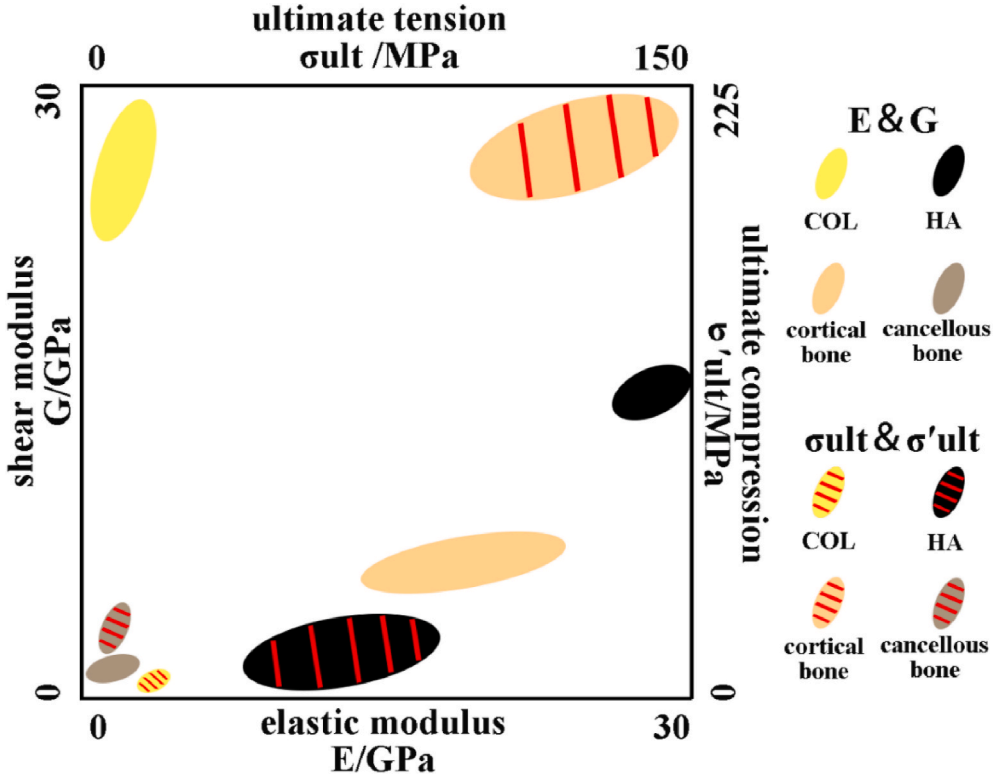

Fig. 1. Mechanical properties of COL, HA, cortical bone and cancellous bone. COL and HA have good toughness and strength respectively, while bone tissue exhibits the characteristics of both materials, showing excellent mechanical properties.

view of the problem of other scaffolds, mineralized collagen scaffolds (MCSs) are ideal candidates for bone repair [67,68]. In addition to simulating natural bone tissue in structure, the MCSs can be reprocessed functionally to promote performance in repairing bone defects. The physical and chemical properties of MCSs, such as their morphology, composition, cross-linking, and mechanical environment, affect repair of bone defects. In addition, the addition of different types of cells and growth factors gives the scaffolds more diversified functions. The synergy of these critical factors promotes MCSs play a more important role in osteogenesis. The MCSs mimic the structure and composition of natural bone, adds appropriate cells and growth factors to build a like-ECM environment, which exhibits pleasant bone repair performance, as shown in Fig. 2. Compared with the composite scaffolds of other materials, MCSs are compatible with natural bone in composition, imitate bone structure and exhibit good bone repair potential. Therefore, mineralize COL was chosen to fabricate the MCSs with better mechanical properties.

In this review, we aim to summarize the state of the art of MCSs as tissue-engineered scaffolds for acceleration of bone repair, including their fabrication methods, critical factors for osteogenesis regulation, current opportunities and challenges for the future. First, the recent progresses in fabrication methods for building the MCSs with high bionic construction of natural bone tissue from traditional strategies to emerging three-dimensional (3D) printing techniques are recommended in detail. Meanwhile, various regulation approaches from physical, biological and chemical aspects are presented for enhancement on the osteogenesis of MCSs. Besides, the opportunities and challenges associated with MCSs as bone tissue-engineered scaffolds are further discussed to point out the future directions for building the superior MCSs.

2. Fabrication methods of MCSs

For bioactive scaffolds, they should have osteogenic properties (induce intracellular and extracellular reactions), and bone conduction properties (provide biocompatible surfaces for bone cell migration). Different fabrication methods provide multiple ways of combining COL and minerals to obtain MCSs that are similar in composition and structure to natural bone and exhibit excellent bone repair performance. Although the structure and morphology of MCSs fabricated by different methods are diverse, they all play an important role in osteogenesis. In this review, traditional methods to fabricate MCSs were divided into two types: direct mineral addition and in-situ mineralization. In addition, 3D printing technology as the most innovative manufacturing method was highlighted, which recently attracted widespread attention in the field of bio-manufacturing. In the direct mineral addition method, mineral substances (such as HA particles) were directly added to COL solution, and then MCSs were obtained by different molding methods. The in-situ mineralization method mixed mineral ions with COL solution, and then form minerals by in-situ deposition. In addition to effectively combining COL and apatite crystals, 3D printing technology control fibers regular arrangement in scaffold, which is the unique advantage over other fabrication methods.

2.1. Direct mineral addition method

According to the mainly ways in fabrication process, direct mineral addition method can be divided into three types: electrospinning, freeze-drying and coating methods. The three specific fabrication methods are shown in Fig. 3.

2.1.1. Electrospinning method

Electrospinning technology refers that the nano- or microfibers obtained by jets from solution or melt under the electric field action [69,70]. Electrospinning scaffolds are widely used for their advantages, such as large surface area-to-volume ratio, high porosity, similar mechanical properties and morphology to ECM [71,72]. Therefore, electrospinning is commonly used in tissue engineering and regenerative medical field.

The mineralized COL fiber was used to reinforce PLA-based scaffold and compared performance with unmineralized scaffolds. The HA nanoparticle was added to COL/PLA solution and ultrasonically shaken to make the mixture was homogenized. The mixed solution electrospun to fabricate mineralized HA/COL/PLA composite scaffold. The addition of mineralized COL fibers significantly increased the fiber network, effectively improved the tensile strength, altered the fiber's degradation behavior and accelerated the degradation rate of composite scaffold [73]. In addition, the HA/COL/PLA scaffold exhibited good cell compatibility with bone mesenchymal stem cells (BMSCs) and human gingival fibroblasts (HGF) cells and satisfied the requirements of "biological evaluation of medical devices" in the process of biosafety evaluation.

The polylactic acid composite (PLA/HA) solution mixed with COL solution and electrospun to fabricate the MCS (HA/COL/PLA) [74]. The performance was compared with pure PLA scaffold and PLA composite (HA/PLA) scaffold. The HA/COL/PLA scaffold showed better adhesion and proliferation on human fetal osteoblasts (hFob), and calcium deposition was the most obvious. These indicated that the HA/COL/PLA

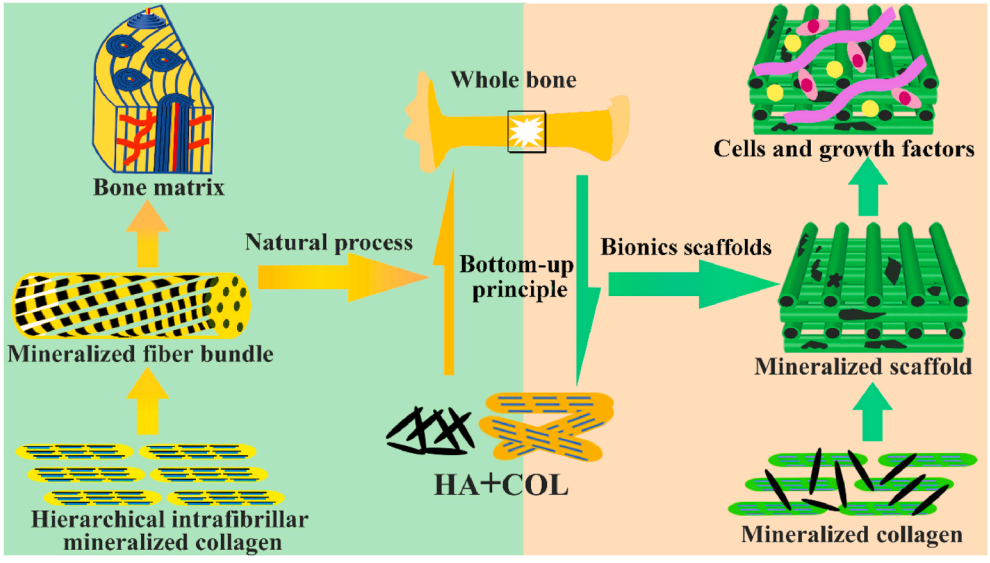

Fig. 2. The natural bone formation process and the bionic strategy of bone repair scaffold. The new bone formation process follows a bottom-up principle. The hierarchical intrafibrillar mineralized COL are formed by HA and COL and serve as substance for next level, which is an important manifestation of bone hierarchical structure from micro to macro. The hierarchical intrafibrillar mineralized COL undergoes rearrangement and assembly to form fiber bundles. The mineralized fiber bundle is the basic unit of bone matrix and provides the necessary spatial structure for bone formation. The bionics scaffold is fabricated by simulating the process of natural bone formation and provided suitable microenvironment to promote bone repair.

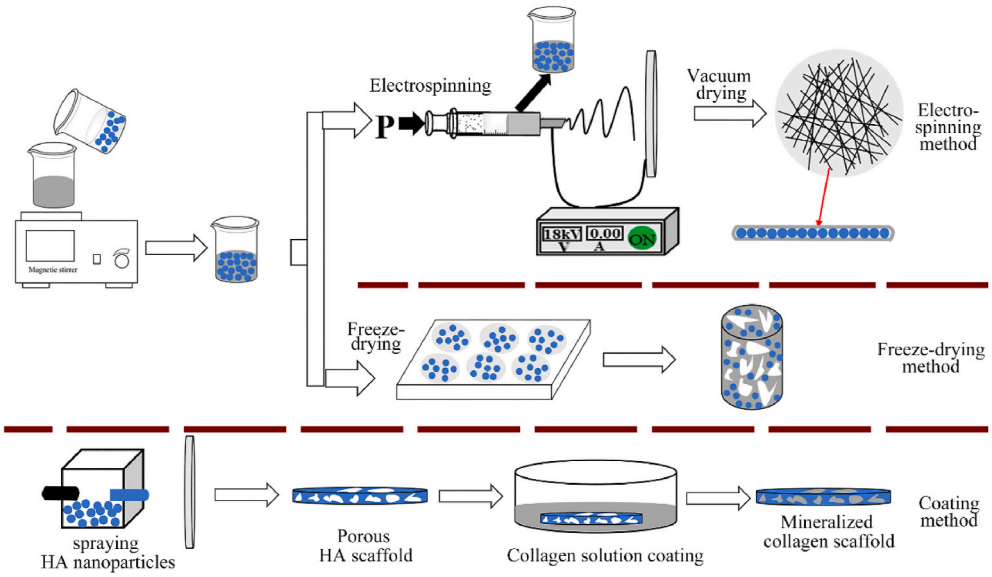

Fig. 3. The illustration of three direct addition methods for fabricating MCSs. The methods of freeze-drying and coating are relatively simple. Compared with these two methods, the scaffold fabricated by electrospinning is made by fibers accumulation, which structure is more similar to the natural bone matrix.

scaffold could be a potential substrate for proliferation and mineralization of osteoblasts than two other scaffolds, which has significance on enhancing bone regeneration.

The Venugopal's group [75–79] also proceeded to a series of studies on MCSs for bone repair. The mainly fabrication method was adding nano-HA particles to COL solution, and then electrospinning to obtain the MCSs. A series of experimental results proved that the MCSs have significantly positive effect on enhanced mineralization. The mineral deposition on MCSs was increased significantly, and mechanical properties were also improved compared with pure polymer scaffolds and composite scaffolds of other materials. The mineralized scaffold also had an important promotion effect on osteoblasts activity, which contributes to the new bone regeneration.

The MCSs fabricated by electrospinning possessed compact structure and suitable porosity for cell penetration, so it is especially profitable for tissue engineering. The electrospinning MCSs have sufficient microporous structure, which can solve the problem of limited space for cell proliferation. The fibers in electrospinning MCSs ranged from nano-to micrometer and reached the fiber diameter of ECM, which is conducive to the cell growth and proliferation. This characteristic of MCSs cannot be achieved by other traditional fabrication techniques and plays an irreplaceable role in the field of tissue engineering and regenerative medicine.

2.1.2. *Freeze-drying method*

The freeze-drying method pretreated model at sufficient freezing temperature to convert the water in gap into ice crystals. The ice crystals sublimated into water vapor at a certain temperature and pressure. Then the residual solution was removed to obtain porous scaffolds [80]. Although the treatment process was simple, its low-temperature characteristic was beneficial to protect the collagen structure from damage, so it was also used to prepare the MCSs.

The MCSs fabricated by freeze-drying method with different mineral contents [81]. The HA particles were added to COL solution, then the mixed solution was freeze-drying. All group scaffolds were cross-linked and sterilized using dehydration heat treatment. The improvement of MCSs mechanical properties was related to the increase of HA incorporation and further amplified by cross-linking treatment. The addition of HA provided excellent function of cell adhesion and osteogenesis and promoted early expression of osteogenic markers and cell-mediated mineralization. These results indicated that the MCSs fabricated by incorporating non-aggregated HA nanoparticles have great osteoinductivity and can be used in bone repair and related fields.

The mineralized composite scaffold applied to the critical skull defect model of New Zealand white rabbits, which was fabricated by directly adding β-TCP to COL solution [82]. The COL/β-TCP scaffolds showed better bone repair effect than pure COL scaffold and significantly improved the differentiation of mesenchymal stem cells to osteoblasts. The COL/HA suspension was poured into molds and lyophilized at a low temperature. The resulting samples were dehydrated in ethanol to remove ice crystals and dissolve mold materials. Finally, the liquid carbon dioxide was used only for drying scaffold to obtain the porous MCSs. The microstructure, biodegradation and mechanical properties of MCSs can be effectively improved by adjusting experimental parameters [83].

The COL gel and HA powder mixed in different ratios to achieve composite gel, which was dried in air and then freeze-dried to fabricate MCSs. The density and porosity of MCSs changed with different mineral ratios and initial air-drying time. The maximum porosity reached 97%, and the minimum reduced to 27% [84]. The MCSs with different morphology and specific porosity/density could be easily obtained by freeze-drying method, which achieved the performance requirements of scaffolds for bone defects under different conditions.

The fabrication process of freeze-drying method is simple, while requires additional treatment to obtain the MCSs with exceptional bone repair effect. The MCSs fabricated by this method mostly are loose porous structure. This method can control internal structure and porosity of scaffold, but there is yet no consensus on concrete action model and quantitative parameters. The MCSs performance can be further optimized by adjusting content and type of mineral and processes of pretreatment and drying. These researches provided reference value for the optimal morphology and porosity of MCSs, which reveal better bone repair performance.

2.1.3. *Coating method*

This method refers to coating another material on the substrate surface to enhance adhesion and cohesion. This biocompatible coating treatment improved biological behavior of the composite scaffold. The MCSs fabricated by coating method through immersing the pre-fabricated HA scaffold into COL solution. The COL fiber penetrated complete HA scaffold and attached to the inside and outside.

The HA liquid precursor deposited on a substrate by plasma spraying

process and then modified the porous apatite coating with COL, COL/rhBMP-2 and COL/RGD solutions, respectively [85]. The adhesion, proliferation and differentiation of mesenchymal stem cells on MCSs were significantly improved. The additional incorporation of rhBMP-2 and RGD further enhanced the proliferation and differentiation of mesenchymal stem cells. The vivo experiments showed that rhBMP-2 has obvious ectopic bone formation and accelerated bone growth effect. The reason why MCSs fabricated by COL-coated HA-precipitated represent excellent osteogenesis is that COL was the effective carrier for osteogenic proteins.

The mixed powder of HA and titanium dioxide sprayed onto the pre-sandblasted Ti6Al4V substrate. The sprayed samples executed alkaline treatment to increase the –OH concentration of surface. The scaffold then soaked in acidic COL solution, so that COL bonded to the -OH on HA surface. The COL fiber adhered well on MCSs surface, which is conducive to cell adhesion and differentiation compared with scaffolds treated by other processes [86].

The coating method is adopted by researchers due to its simple fabrication process. The MCSs fabricated by COL-modified HA not only bionic natural bone in composition and morphology but also enhance bone integration and early fixation of bone-implant interface. However, the amount of COL deposited in apatite-base scaffold by this method is restricted. This is an urgent problem that restricts its further application in the bone repair field. How to strengthen the combination of COL and HA in MCSs and obtain a suitable organic/inorganic ratio are problems that restrict development of coating method.

The MCSs fabricated by different ways of direct mineral addition method showed the effect of promoting bone repair. The main difference of MCSs was reflected in the micro-morphology, as shown in Fig. 4. The MCSs showed nano-fibers structure fabricated by electrospinning method, porous thin layer structure by freeze-drying method, and sheet structure with particles attached by coating method. The MCSs with different structure exhibited the ability to promote bone cell adhesion, proliferation and differentiation. These indicated that MCSs fabricated by direct mineral addition method has an excellent potential of bone repair.

2.2. *In-situ mineralization method*

The in-situ mineralization method refers that adding calcium and phosphate ions rather than mineral crystals to the COL solution system or immersing the prefabricated COL scaffold into a solution containing two mineral ions. Mineral ions are deposited on COL fibers and gradually crystallize and grow in this method. This in-situ mineralization is more similar to the mineral forming process of natural bone, so the scaffold's structure is closer to natural bone. This is the reason why this method is most used for fabricating bone repair scaffolds. This paper divided in-situ mineralization method into five categories according to

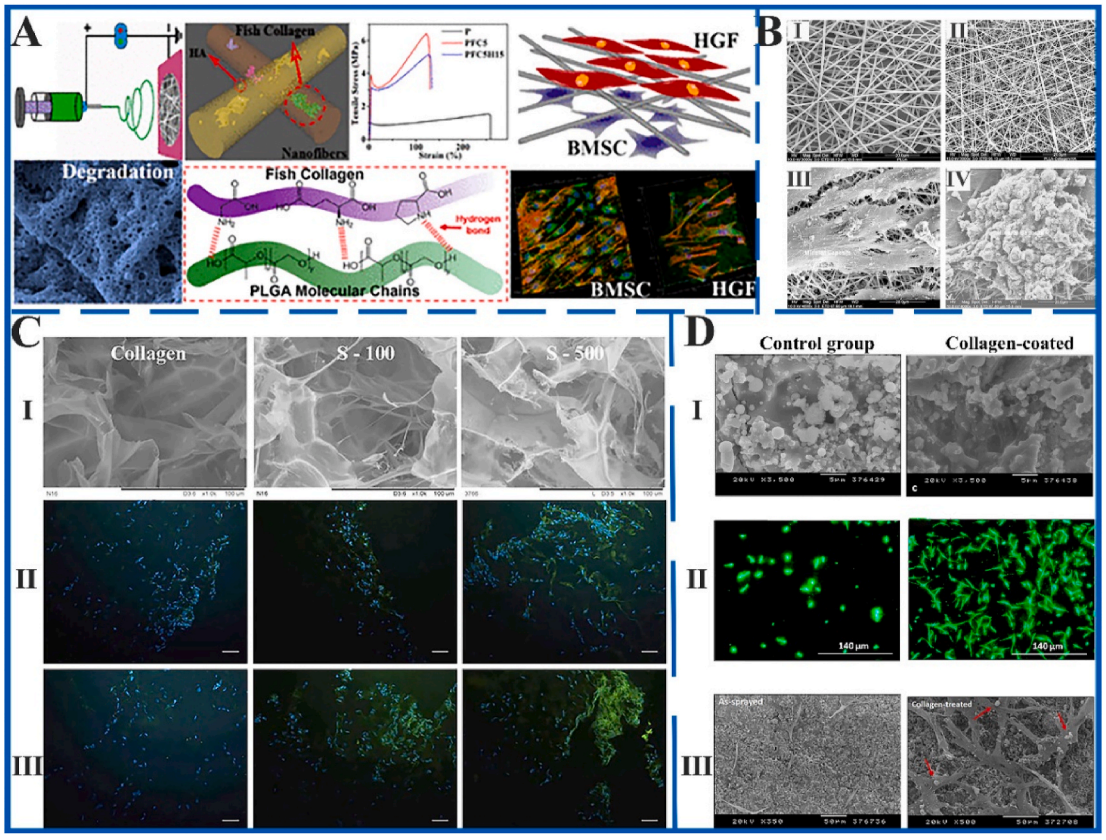

Fig. 4. The morphology of MCSs fabricated by electrospinning (A and B), freeze-drying (C) and coating (D) methods and the results of bone cell culture *in vitro*. A: The schematic diagram of fabrication strategy, morphology and cell compatibility of HA/COL/PLA composite scaffold. The MCSs significantly improved mechanical properties and exhibited excellent cell compatibility. Figure from reference 73. B: SEM images of electrospun I) PLA, and II) HA/COL/PLA scaffold. The hFob interaction with III) PLA and IV) HA/COL/PLA nanofibrous substrate after culturing 20 days. The HA/COL/PLA scaffold is more advantageous to cell adhesion and proliferation on hFob. Figure from reference 74. C: The COL, S-100 (1:1 HA/COL), and S-500 (5:1 HA/COL) scaffolds fabricated by freeze-drying method. I) The SEM images of three scaffolds. Three scaffolds promoted earlier expression of II) osteopontin and III) osteocalcin at day 14. The MCSs considerably promoted the markers' expression of bone formation. Scale bar = 100 μm. Figure from reference 81. D: The HA, HA-COL scaffolds fabricated by coating method. The control group not executed alkali treatment and collagen coating. I) Surface of two scaffolds. II) the fluorescent live/dead staining of osteoblasts at 7 days. III) morphology and distribution of osteoblasts on two scaffolds at 7 days. The COL-coated group had an observable effect on promoting osteoblasts proliferation, differentiation and mineralization than the control group. Figure from reference 86.

the different treatment process: self-assembly, electrodeposition, vesicle deposition, vapor deposition and multi-process methods. The illustration of in-situ mineralization method is shown in Fig. 5.

2.2.1. Self-assembly method

The self-assembly concept proposed by Grzybowski refers that the components automatically organize into patterns or structures without human intervention [87]. This method is widely used in the entire natural and technical field. The highly hierarchical mineralized intrafibrillar (HMI) apatite nanocrystals can be assembled within reconstituted type I COL fibrils using self-assembly approach [88]. The MCSs fabricated by self-assembly exhibited potential of delivering growth factors in bone regeneration field.

The simulated body fluid (SBF) mixed with COL solution and adjusted the pH to incubate samples at room temperature. The COL fibers self-assembled to form mineralized COL hydrogel, which was then compressed and freeze-dried to obtain the MCSs [89]. The MCSs obtained by this method exhibited excellent biocompatibility *in vivo* and *vitro* and promotion on cell proliferation. In addition, the MCSs exhibited hierarchical structure for presence of template analogs. This structure had significantly reference value for preparing scaffold, which is similar to natural bone in structure.

Pure COL scaffold is immersed in SBF containing Portland cement to fabricate the mineralized scaffold [90]. The role of sequestration and temptation analogs was also explored in COL mineralization process. When polyacrylic acid (PAA) existed as sequestration analogs, calcium and phosphate ions chelated into the transient ACP nanophase. Without sequestration analogs, sodium trimetaphosphate (STMP) and sodium tripolyphosphate (STPP) as the temptation analogs leaded extrafibrillar precipitation of apatite, which randomly oriented along the COL fibril surface. The sequestration analogs and temptation analogs be employed together to form intrafibrillar mineralized COL, which is very similar to natural bone structure. The PAA and STMP/STPP were used as double bionic analogs to prepare hierarchical intrafibrillar mineralized collagen scaffolds (HIMCSs), which have significance for understanding the mineralization process in natural bone.

In order to explore the role of non-COL protein (NCP) in mineralization process, The PAA as the NCP analogs to fabricate HIMCSs, nonhierarchical intrafibrillar mineralized collagen scaffolds (NIMCSs) and extrafibrillar mineralized collagen scaffolds (EMCSs) [91]. The HIMCSs provided optimal microenvironment to regulate osteoblastic differentiation of stem cells and proper degradation rate for new bone ingrowth than other scaffolds. The bone regeneration is significantly improved via the hierarchical nanostructure, which was similar to natural bone. Distinct nanometer-scale surface topographies of different MCSs were the key element to modulate stem cell fate. This is useful

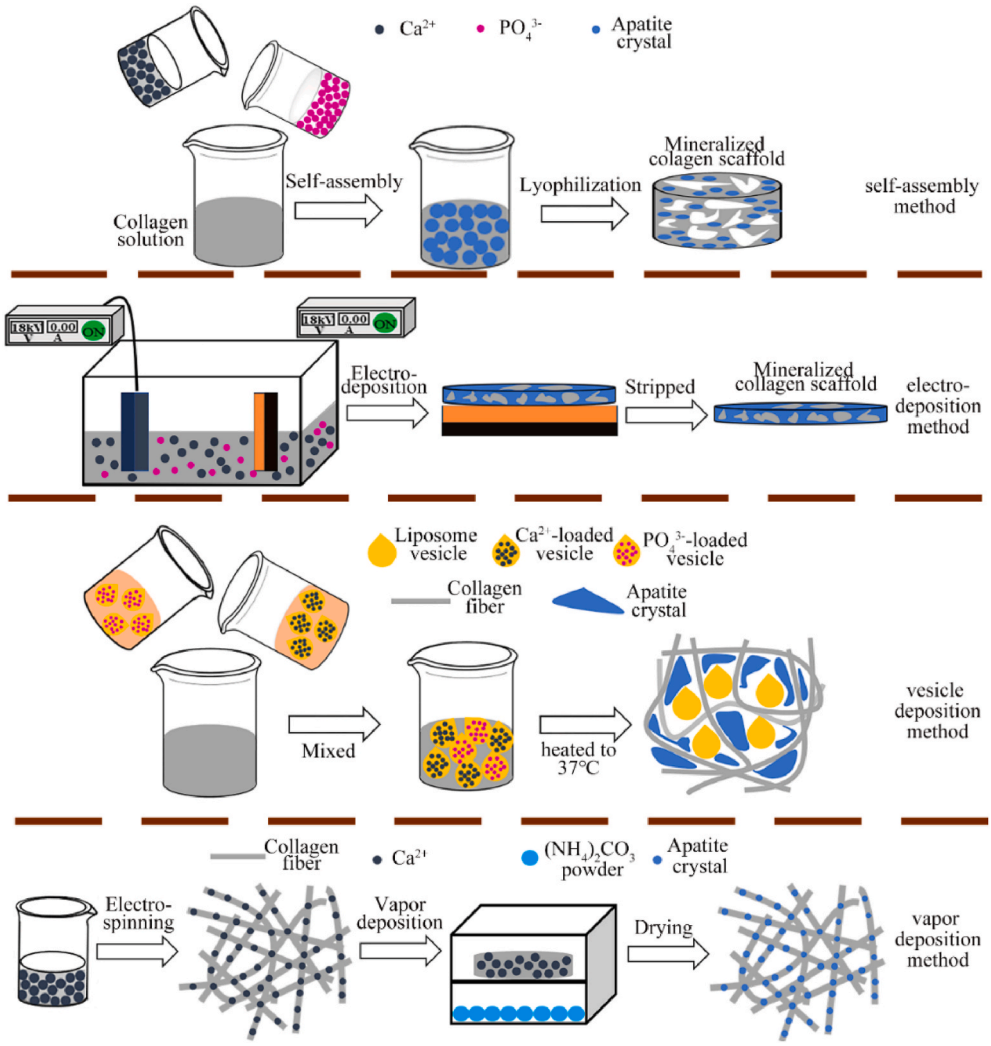

Fig. 5. The illustration of in-situ mineralization method for fabricating MCSs. Self-assembly, electrodeposition and vesicle deposition methods fabricated MCSs through COL and mineral co-precipitation. Vapor deposition prefabricated the COL scaffold chelated with calcium ions, then provide other mineral ions by vapor deposition.

both in understanding the mechanism of natural bone mineralization and identifying important bio-properties of hierarchical nanostructures.

For fabrication of MCSs by self-assembly method, the Cui group of Tsinghua University did a series of researches. Cui et al. [92–95] added calcium ion solution and phosphate solution to dilute COL solution and then adjusted the pH to neutral. The precipitates were collected by centrifugation and freeze-dried to obtain MCSs. In results of the high-resolution transmission electron microscope, it can be observed that the mineralized COL fibrils are arranged in parallel with each other, and HA crystals grow on the surface of these fibrils. The COL/HA composite scaffold fabricated by self-assembly holds the like-bone hierarchical structure.

The ampholyte carboxymethyl chitosan (CMC) also stabilized amorphous mineral particles under acidic conditions and doped the biologically active elements strontium or silver into collagen fibers to realize the synergy of collagen self-assembly and mineralization [96]. This strategy fabricated strontium-doped collagen scaffolds (Sr-CS) with both osteogenic and osteoimmune induction effects, and silver-doped collagen scaffolds (Ag-CS) with antibacterial effects. Mineralization of fibrillar COL with bionic process-directing agents enabled scientists to gain insight into the potential mechanisms involved in intrafibrillar mineralization. In addition to the factors mentioned above, the balance between osmotic equilibrium and electroneutrality is also notable for self-assembly mineralization in COL fiber [97]. This theory establishes a new model for COL intrafibrillar mineralization that supplements existing COL mineralization mechanisms, but the specific role has not been thoroughly studied yet.

2.2.2. Electrodeposition method

Electrodeposition was a high-speed and effective method for fabricating MCSs. It required that the mineral exists in electrochemical cell in the form of ions [98]. When the appropriate voltage or current was provided, mineral ions will be deposited on the corresponding base plate to form scaffold. The electrodeposition strategies to fabricate MCSs not demanded harsh conditions, and the choice of dissolution was broader [99]. In addition, the electrodeposition method allowed a variety of materials deposited on a substrate to form the complex scaffold with multi-functional and different nanostructures, which can be developed by changing experimental parameters [100,101].

The appropriate amount of $Ca(NO_3)_2$ and $NH_4H_2PO_4$ was dissolved in distilled water as the electrolyte, and then added soluble type I COL solution. The current of 34 mA was implemented at room temperature to form the COL/calcium phosphate (CaP) composite scaffold on the cathode plate [102]. The mineral crystals in scaffold surround COL fibers, which are partially calcified during the assembly of COL molecules. The MCSs fabricated by electrodeposition had strong ability to bind fibronectin and bioactive surface that promote bone formation and implants fixation. The MCSs also had metal chip load capacity, which will play a major role in the medical equipment field.

The CaP/COL scaffold was deposited on a carbon-based substrate by using the electrochemically assisted deposition method. The COL solution was added to electrolyte with calcium and phosphate ions. The CaP/COL composite scaffold was fabricated under constant current and immersed in $Ca(OH)_2$ solutions. The MCSs represented three-dimensional network structure, and the CaP aggregates were evenly spread on COL network. With the COL concentration increased, the mechanical properties of scaffolds also improved [103].

The electrodeposition method exhibited many advantages, such as easily control process, low fabricated temperature, and suitability for complex implant geometries. When it was utilized to fabricate the MCSs, mineral crystals evenly spread on COL network and effectively solved the problem of mineral aggregation. This method also provides a good choice for fabricating MCSs with uniform mineral distribution.

2.2.3. Vesicle deposition method

During the bone formation in some parts of human body, HA crystals are derived from calcium and phosphate ions deposited in non-cellular liposomes vesicles. Liposomes are continuous, closed, round vesicles formed by one or several layers of phospholipids dispersed in an aqueous medium. Nanoliposomes are naturally soft nanoparticles with biocompatibility, biodegradability, easily preparation, handling and decoration, and low toxicity, which have been widely used in drug and gene delivery, and tissue engineering. In order to simulate the mineralization process in nature, some researchers proposed to encapsulate calcium and phosphate ions in vesicles. These liposomes vesicles were embedded in ECM and mainly composed of COL [104,105]. Different driving strategies were then used to release mineral ions and mineralize them in the matrix. The MCSs fabricated by vesicle deposition not only supplied excellent bone repair scaffold, but also provided a new perspective for understanding the collagen mineralization process.

The calcium and phosphate ions were encapsulated in the lipid mixture consisting of dipalmitoylphosphatidylcholine (90 mol%, DPPC) and dimyristoylphosphatidylcholine (10 mol%, DMPC). Then the liposome vesicles were added to COL solution and heated to 37 °C to obtain the mineralized COL gel scaffold. The minerals were distributed in COL matrix in the form of single particles or mineral aggregates, which was formed by the liposomes release of calcium and phosphorus ions. In addition, the minerals exhibited a certain orientation along the COL fiber surface. This strategy encapsulated mineral ions in the temperature-sensitive liposomes vesicle and then released under the action of thermodynamic force [106]. Two mineral ions released and combined with COL gel to fabricate the mineralized COL gel scaffold. This heat-driven vesicle mineralization method has a great potential in the injectable medical materials field and provides new solution for minimally invasive reconstruction of bone and tooth tissue.

The liposome vesicles used for biofabrication of MCSs have some advantages that other methods do not have. It cannot only obtain mineralized fibers with a certain orientation, but also provide unused research method for the mineral deposition during the new bone formation. The mineralized collagen material obtained by this method has higher fluidity, so it can be used as an injectable material to fill specific defect sites. At the same time, the mineralized collagen gel is also a safe drug or protein supporter. The drug or protein is encapsulated in collagen gel through crosslinking and achieves the effect of controlled release. This collagen gel has thermal response and can control its mineralization process by simple treatment. This simple physical response system has significant development value and can be used in bone repair model, which is low trauma, intelligent release and encapsulated cells and proteins.

2.2.4. Vapor deposition method

Regarding the mineralization process, most strategies provided mineral ions from solution, while some scholars get mineral deposition by gas to achieve the purpose of mineralization. The calcium ions first chelated on COL fibers and another mineral ion was provided by vapor. When the two mineral ions contacted, mineralization process occurred to obtain the MCSs. The vapor deposition method fabricated MCSs with uniform minerals and provided another mineralization research strategy. However, the requirements for minerals were more stringent in this method. It required mineral easily produces gas-phase ions, so carbonate was often selected.

The COL dissolved into the hexafluoroisopropanol (HFIP) solution with calcium ions and catecholamines. The composite solution electrospun under appropriate conditions to fabricate fiber scaffold. The prefabricated COL fiber scaffold was enclosed in a sealed desiccator with $(NH_4)_2CO_3$ powder to fabricate MCSs. The MCSs morphology and better osteogenic properties than the control group were shown in Fig. 6 [107]. There is recognizable mineral precipitation in MCSs, and its excellent mechanical properties achieved the limit of cancellous bone. At the same time, the presence of catecholamines makes the MCSs with photoluminescent properties. Compared with pure COL scaffolds or tissue culture plates, MCSs enhanced Osteoblasts adhesion, penetration,

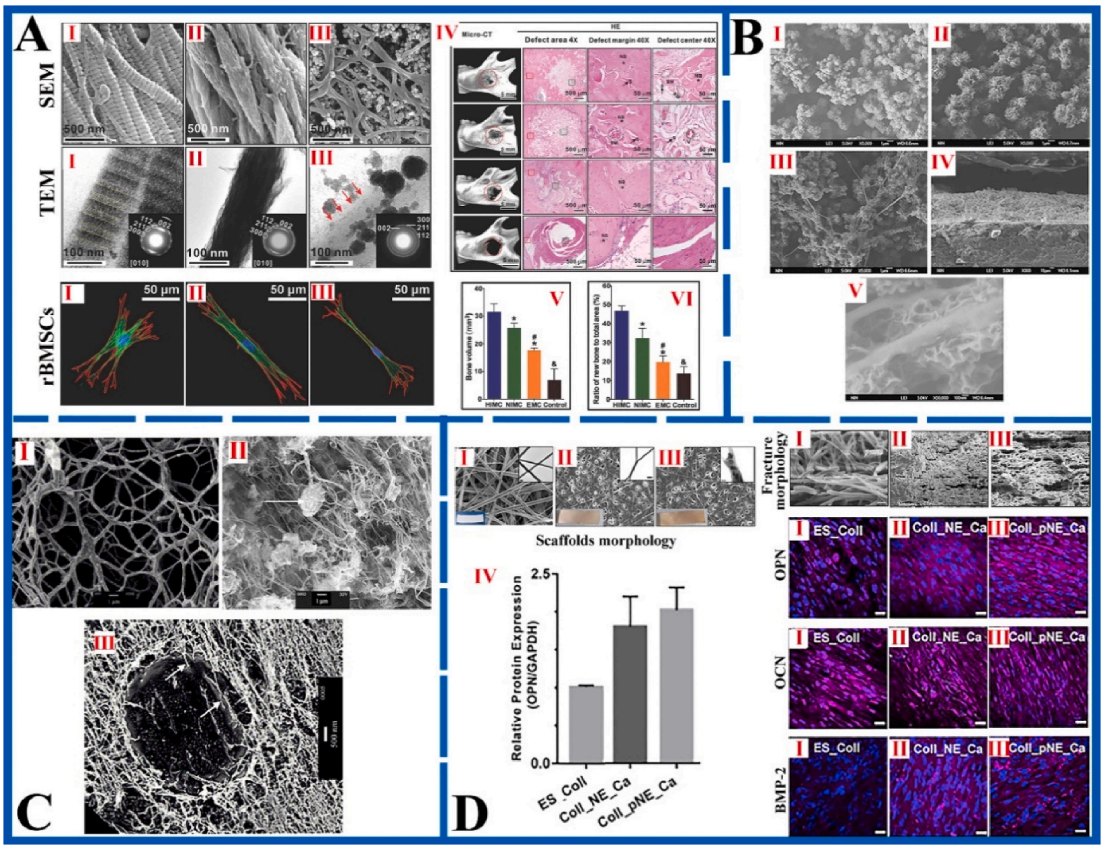

Fig. 6. The morphology of MCSs fabricated by self-assembly (A), electrodeposition (B), vesicle deposition (C) and vapor deposition (D) methods and characterization of bone repair effect. **A:** The SEM image and corresponding unstained TEM images of HIMCSs (I), NIMCSs (II) and EMCSs (III). Rat bone marrow stem cells (rBMSCs) morphology after 1 d of culturing on the I, II and III. The rBMSCs seeded on HIMC showed long filopodia and thick stress fiber formation, which exhibits highly branched "osteocyte-like" shape. IV) Bone regeneration *in vivo* after implantation with I, II and III for 12 weeks. V) Bone volume of the defect area from different groups based on micro-CT test. VI) Semi-quantitative analysis of new bone based on histologic examination. Figure from reference 91. **B:** The morphology of composite scaffold with different COL concentrations: I) without COL, II)100 mg/L, III) 500 mg/L, IV) cross-sectional morphology of 500 mg/L, V) immersed in Ca $(OH)_2$ solution of 500 mg/L. With COL concentration increased, the network structure formed more obvious. After immersing in $Ca(OH)_2$ solutions, the nanofiber structure of MCSs resembled natural bone. Figure from reference 103. **C:** The SEM image of vesicles only containing COL after dried (I). The low magnification SEM image (II) and freeze-fracture TEM image (III) of mineral/COL composite scaffold (COL concentration = 3.22 mg/ml, $[Ca^{2+}]$ = 26 mM, [P] = 25 mM). The composite scaffold is composed of COL fibers and apatite crystals attached to the surface of vesicle. Figure from reference 106. **D:** The scaffold's morphology and expression of osteogenic proteins by hFob cells seeded on scaffolds. I) pure COL scaffold (ES_Coll), II) composite scaffold containing norepinephrine (NE) and Ca^{2+} (Coll_NE_Ca), III) mineralized scaffold fabricated by vapor deposition (Coll_pNE_Ca). The MCSs obtained by vapor deposition method showed extensive roughness and ripples, which indicate that its tensile strength, hardness and toughness increased significantly. The expression of osteocalcin (OCN), osteopontin (OPN), and bone matrix protein 2 (BMP-2) in mineralized scaffold increased meaningfully, which indicates that it has a better performance for new bone formation. Figure from reference 107.

proliferation and differentiation, and osteogenic gene expression for hFob.

The vapor deposition method for fabricating MCSs has been limited in mineral selection. The traditional phosphates difficult exist in gas form, so carbonate often used in the mineralization process as a substitution. Appropriate selection range of mineral ions has great significance to broaden the application fields of vapor deposition method.

2.2.5. *Multi-process method*

The MCSs obtained by a single fabrication method usually not satisfy all requirements in actual condition, so it is necessary to combine multiple process methods used together. The MCSs fabricated by combination method of electrospinning and freeze-drying, which composed of nanofiber structure and represented uniform mineral distribution. The MCSs fabricated by combination method of self-assembly and 3D printing exhibited specific shape and hierarchical structure. The ideal tissue engineering scaffold fabricated by multi-process method, which exhibits the characteristic of different MCSs. However, how to combine different fabrication processes and choose appreciate method to combine are problems that are taken into account by researchers. In the following, the MCSs fabricated by multi-process method will be briefly introduced to provide reference for more researchers.

The calcium and phosphate ions were added into gelatin solution respectively, and then mixed to precipitate HA/gelatin matrix. After freeze-dried, the matrix was redissolved in organic solvent and electrospun under controlled conditions to obtain mineralized gelatin fiber scaffold [108]. Combining the freeze-drying and electrospinning method, mineralized gelatin scaffold represented similar internal structure to natural bone, which fabricated by HA crystals evenly distributed in the gelatin matrix. When this scaffold used for bone repair research, it was found that the MCSs had better bone-derived cellular activity and more obvious bone repair effect than the pure organic polymer scaffold. This method could produce biomedical scaffolds with controlled gradients, so its potential for guiding tissue regeneration is huge.

The MCSs with isotropic equiaxed structure or unidirectional laminar structure fabricated by combining self-assembly and freeze-casting methods. The COL solution was put into modified-SBF (*m*-SBF) for in-situ precipitation of apatite crystals. The precipitate was taken out and controlled freezing-casting to obtain MCSs. The scaffold contained

bone-shaped apatite nanoparticles, and the mineral content could be controlled by adjusting initial amount, up to 54 wt% [109]. In the mouse model of cranial skull defect, it was found that the scaffold has excellent support for new bone formation. The formation mechanism of equiaxed and hierarchical scaffolds was studied, and the freezing mechanism of equiaxed and hierarchical solidification was also established.

The MCSs also can be fabricated by method of alkaline phosphatase-catalyzed calcification [110]. Alkaline phosphatase coated on COL scaffold as the source of phosphate. The pretreatment scaffold then hydrolyzed in solution with calcium ions to generate apatite deposition. Eight to ten layers COL/CaP scaffold were obtained through multiple coating and mineralization. This MCSs exhibited favorable mechanical strength and maintained translucency and flexibility in the air. This composite scaffold also represented stability in water, which promote adhesion and proliferation of fibroblasts.

The single fabrication technology is difficult to satisfy construction of complex bionic structures *in vitro*. Therefore, the combination of different technologies was regarded as a clear and necessary emerging trend in biofabrication field. The multi-process fabrication method can develop scaffolds with more bionic characteristics and structures. For example, the porosity of the scaffold increased without affecting the biomechanical properties and biocompatibility [111]. It is conducive to the further development of tissue engineering to choose the appropriate method according to different requirements.

The MCSs fabricated by different in-situ mineralization methods also showed differences in morphology, but all have the effect of promoting bone repair, as shown in Fig. 6. The in-situ mineralization method for fabricating MCSs was more in line with the natural bone formation process, so the hierarchical intrafibrillar mineralized structure in collagen was obtained, while this effect could not be obtained by the direct mineral addition method.

2.3. 3D printing method

3D printing, also known as additive manufacturing technology, includes different methods of powder-based 3D printing (3DP), stereolithography (SLA), fused deposition modeling (FDM), selective laser sintering (SLS) and extrusion printing [112–114]. Compared with the traditional method introduced above, the unique advantage of 3D printing method is that can precisely control the fiber arrangement [115–117]. 3D printing refers to setting up the certain trace in advance according to required model, and then printing to get the scaffold with specific shape [118]. In the fabrication process of MCSs, extrusion printing is usually used, which has the advantages of realizing customized shapes, precise pore size control, high pore interconnection rate, and rapid production [119–121]. The MCSs fabricated by 3D printing method not only fulfil the unique shapes requirements of bone defect parts, but also have more controllability in the microstructure. With the improvement of tissue engineering technology, in addition to printing simple biological scaffold, more researchers have turned their attention to print complex biological structures [122–124]. The complex systems of micro-tissue structures or organoid morphology, which combine cells, growth factors and other substrates with scaffold materials, will play an extremely important role in regenerative medicine [125,126]. The tendency is same for development of bone repair, which from pure scaffold to complex biological scaffold loaded with cells. 3D printing is an important method in fabricating tissue engineering scaffold, the illustration of 3D printing method for fabricating MCSs was shown in Fig. 7. Next, the 3D printing method for fabricating MCSs will be introduced.

The triple helix structure of COL is untwisted at 40 °C, so the fabrication of COL scaffolds required printing at room temperature or even low temperature. Pei et al. [127] individually homogenized COL and HA in acetic acid solution and mixed the two slurries to produce printing ink. The printed scaffold was further cross-linked to improve its mechanical properties and sterilized with ethylene oxide for subsequent experiments. The MCSs exhibited an excellent 3D structure, maintained raw material properties after printing, promoted the proliferation of bone marrow stromal cells *in vitro* and improved the osteogenesis, as shown in Fig. 8. This low-temperature 3D printing strategy can incorporate a variety of active factors into the mineralized scaffold. This research provided a bio-manufacturing method, which not damage the material's biological activity. It will be widely used in the field of tissue engineering and organoid manufacturing.

Directly 3D-printed CaP scaffold and then coating the COL layer, which method also fabricated MCSs with excellent bone repair performance. The CaP powder and acid binder solution (phosphoric acid diluent) were used for printing. The printed scaffold quickly immersed in 0.1 wt% phosphoric acid solution, and then washed in deionized water to improve the surface adhesion and remove residual acid solution. The pretreated scaffold immersed in COL solution, so that it coated with COL. Finally, the MCSs obtained by air-dried and sterilized. The COL coating can significantly improve the maximum bending strength and cell viability of MCSs [128]. The MCSs also showed bone conductivity, which can promote new bone growth.

Deproteinized bovine bone (DBB) particles as an additive promoted the bone repair performance of scaffold. The HA and DBB particles were respectively added to acidic COL solution to prepare bio-ink. The two kinds of MCSs obtained by freeze-drying, crosslinking, washing and freeze-drying again. Pure COL scaffold was fabricated by the same process as control group. The two mineralized scaffolds both exhibited porous structure, and HA/COL scaffolds showed better mechanical properties than DBB/COL scaffolds [129]. This was because HA particles are smaller and more evenly distributed on COL surface. Compared with pure COL scaffolds, the MCSs were more excellent in inducing osteogenic gene expression and cell proliferation. The physicochemical and biological properties of MCSs fabricated by 3D bioprinting were suitable as porous bone substitutes, which plays an important role in the field of specific shape bone defects.

In addition to MCSs, the extra cells also play an important role in bone repair. Due to its unique low-temperature fabrication strategy, 3D

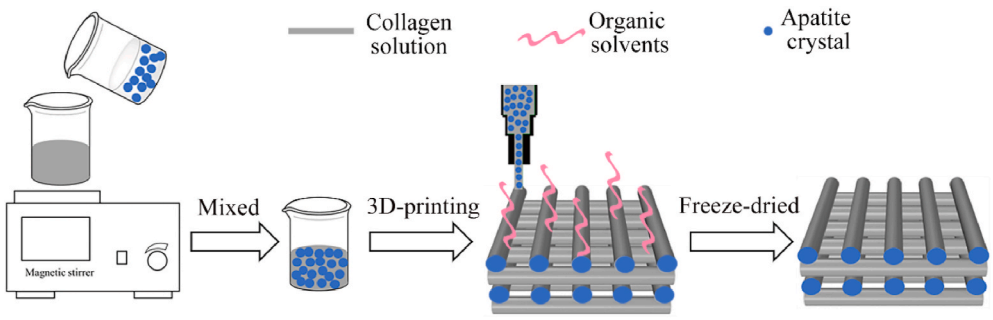

Fig. 7. The illustration of 3D printing methods for fabricating MCSs. The COL and apatite particles mixed and printed at a low temperature to prepare MCSs containing mineral crystals in fibers.

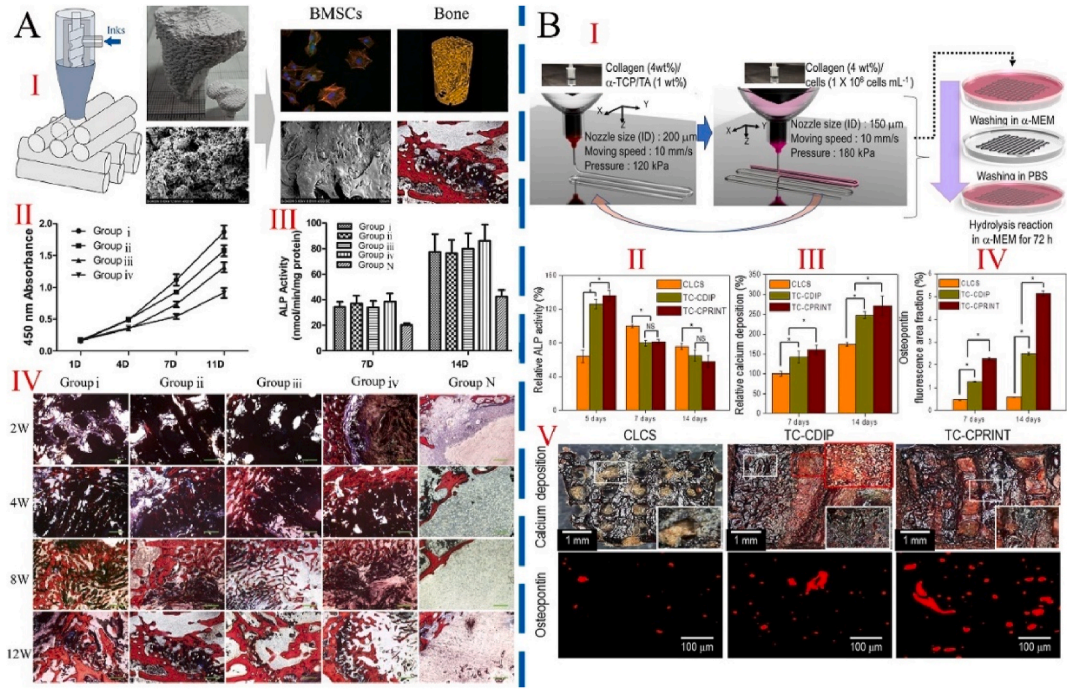

Fig. 8. The cell-free and cell-containing 3D printed MCSs and their effects on bone repair *in vivo and in vivo*. **A**: The cell-free MCSs fabricated by Low-temperature 3D printing method. I) Schematic diagram of preparation strategy and effect of bone repair *in vivo*. II) Measurement of BMSC proliferation on scaffolds using the CCK8 assay at 1, 4, 7, and 11 days after seeding. III) ALP activity of BMSCs on scaffolds 7 and 14 days after seeding. IV)Histological analysis of new bone formation around and within the scaffolds in the rabbit femoral condyle defect model. Group i-iii represented 3D printed scaffold with various rod widths. Group iv represented nonprinted scaffolds. Group N was the control group, which cultured cells with osteoinductive medium but not seeded on a scaffold. After Van Gieson staining, newly formed bone stains red; the tissue stained dark blue is fibrous tissue. Scale bar: 100 μm. The interconnecting pores within the printed scaffolds facilitated cell penetration and mineralization before the scaffolds degraded and enhanced repair. Figure from reference 127. **B**: Fabrication schematics and osteogenic activities of cell-loaded scaffolds. I) a 3D cell-laden α-TCP/collagen scaffold using cell printing. II) Relative alkaline phosphatase (ALP) activity. III) Relative calcium deposition and IV) relative area of OPN images of scaffolds (n = 5). V) Optical images of Alizarin Red S (ARS) and osteopontin (OPN) staining of the scaffolds after cell culture for 14 days. CLCS: cell-laden collagen scaffold. TC-CDIP: 3D α-TCP/collagen scaffold was dipped into a cell-laden collagen solution. TC-CPRINT: the cell-laden collagen solution was printed onto 3D α-TCP/collagen scaffold and repeated several times. The cell-loaded scaffold demonstrated significantly higher cellular activities, including metabolic activity and mineralization, compared with the control group. Figure from reference 130.

bio-printing technology can print COL ink loaded cells, as shown in Fig. 8. The cell-loaded α-TCP/COL scaffold fabricated by a two-step 3D printing method. The COL solutions containing α-TCP and cells were printed layer by layer alternately. Finally, the scaffold was cultured in medium and washed in phosphate buffer saline (PBS). Compared with the cell-loaded scaffold by simple impregnation, the 3D printed cell-loaded α-TCP/COL scaffold exhibited better osteoblast activity and mineral deposition [130]. This indicated that the MCSs have potential for bone repair application. In addition, the change of control parameters during printing process showed an impact on scaffold morphology, such as the diameter of printing nozzle, air pressure, and ink characteristic. The scaffold possessed exact requirements can be achieved by 3D printing method through an appropriate control parameter.

In the field of bone tissue engineering, the main advantage of low-temperature 3D bioprinting was that it can produce polymer-mineral composite scaffolds with specific morphology. In suitable conditions, the printing-ink fabricated scaffold loaded osteoblasts to further promote the bone repair effect. Compared with traditional metal printing or other rapid prototyping technologies, the low-temperature 3D bioprinting has further selection ranges of materials, which has been used to fabricate a variety of composite scaffolds as bone repair materials. Due to its low-temperature properties, low-temperature 3D bioprinting

Table 1
Advantage and disadvantage of different fabrication methods of MCSs.

Fabrication methods		Advantage	Disadvantage	Ref
Direct mineral addition method	Electrospinning method	Fiber diameter is nanometer level	Irregular arrangement of fibers	73–79
	Freeze-drying method	Low temperature; loose porous structure	Simple shapes	81–84
	Coating method	Enhanced adhesion and cohesion	Restricted COL amount	85, 86
In-situ mineralization method	Self-assembly method	Hierarchical mineralized intrafibrillar	Long time; additional analogs	89–95
	Electrodeposition method	Wider application field; uniform mineralization	Surface mineralization	102, 103
	Vesicle deposition method	Heat-driven; safe supporter of drug or protein	Narrow temperature range	106
	Vapor deposition method	Uniform and internal mineralization	Limited mineral sources	107
	Multi-process method	Multiple morphology and functions; satisfy specific requirements	Intractable conflicts in different methods	108–110
3D printing technology		Unique shapes; regular arrangement; precise size control; biofunctionalization	Insufficient printability of ink; thicker fiber diameter	127–130

can compound multiple components such as cells, proteins and minerals. This bionic scaffold at tissue and organ level was the utmost importance for the development of bone tissue engineering.

Different fabrication methods present its unique advantages and disadvantages. Therefore, we summarize and compare the significant advantages and disadvantages of fabrication methods of MCSs in Table 1. Among these methods, the unique advantages of electrospinning and 3D printing are obvious. Electrospinning technology is widely used in the field of tissue engineering because the diameter of its fibers is at nanometer level. While its irregular arrangement restricts its further application. 3D printing technology can perfectly overcome the drawback of fiber arrangement. With the development of 3D printing technology, more suitable bio-inks will be provided, the line will be thinner, and the accuracy of arrangement will be further improved. If advantages of the two methods are combined, MCSs will exhibit more excellent structure and osteogenic properties and play a greater role in bone repair and even biomedical engineering fields.

3. Critical factors in osteogenesis of MCSs

Since the concept of tissue engineering was proposed by Prof. Robert Langer, researchers awarded the importance of synergy between bone-like scaffolds and microenvironment systems, which showed better tissue repair effect [131]. Bone regeneration need four basic conditions: osteoinduction, cell response to osteogenic signals, appropriate ECM environment, and regional vascularization [132]. According to the above four basic conditions, MCSs behave sufficient mechanical support and provide a suitable growth environment for bone regeneration. The critical factors in osteogenesis of MCSs were analyzed from three aspects: physics, biological and chemistry, in order to explore the further effects on bone repair. In these three aspects research, chemistry and biology occupied the majority. As an important manifestation of physics, mechanical action was often ignored before. In the following, the mechanical action was regarded as a single factor in physics and emphasized.

3.1. Physical cues

3.1.1. Mechanical action

Natural bone was the mechanically sensitive tissue that can sense and respond to external mechanical effects [133–135]. Bone cells, including osteocytes, osteoblasts and osteoclasts, were widely studied as mechanical sensors during bone remodeling [136]. These cells constituted the basic multicellular unit in the bone remodeling chamber [137]. In order to respond to external mechanical stimuli in timely and accurate, these cells achieved crosstalk through cell-to-cell contact or transmission of signal molecules [138–140]. Researches evidenced that at the cellular and molecular levels, bone cells and interstitial fluid can also sense and respond to external mechanical loads [141]. During the mineralization process of bone matrix, fluid shear stress (FSS) played the dominant mechanical role [142,143]. Therefore, there is great significance to explore the FSS effect on transformation of mineral crystals and mineralized COL fibers during new bones formation [144].

The Niu group has made a series of studies about the FSS effect on COL fiber mineralization, as shown in Fig. 9. In early stage, the FSS contribution to conversion of ACP to bone apatite was studied [145]. It was found that the application of low FSS has positive effect on transformation of ACP to calcium deficient HA (CDHA), and high FSS has negative impact on this transformation process. When FSS applied to pure COL, the entanglement between COL fiber segments was easier cut and assembled in single direction to form an ordered structure [146]. Next, the authors explored the effect of low FSS on COL mineralization [147]. The calcium and phosphate ion added to diluted COL solution and adjusted the pH to alkaline. Different FSS applied to the composite solution and then freeze-dried precipitate to obtain MCSs. Under the action of FSS, ACP particles were smaller and dispersed in COL fibers, which leads to intrafibrillar mineralization. The 1.5 Pa FSS exhibited positive effect on COL mineralization, which is specifically manifested in the enhanced degree of COL self-assembly, the acceleration of formation and transformation of ACP, and the well-orderly structure and orientation of apatite. In addition to the magnitude of FSS, the effect of different types FSS on COL mineralization was also researched [148]. The COL composite solution was prepared by above way, then applied periodic 1.0 Pa FSS and freeze-dried precipitate to obtain the MCSs. With the loading of periodic FSS, ACP can penetrate in COL fibers and be further transformed into HA crystals. The periodic FSS was conducive to form highly oriented hierarchical intrafibrillar mineralized (HIM) COL. This HIM structure is closer to mineralized COL structure of natural bone.

There is great significance to understand the role of FSS on collagen mineralization. This not only contributes to investigate the mechanism of collagen mineralization, but also guides researchers to fabricate MCSs with HIM structure. The research of FSS effect only reported on mineralized COL level, its effect on whole process of bone regeneration has not been fully reported. In addition, the FSS is mostly suitable for *in vitro*

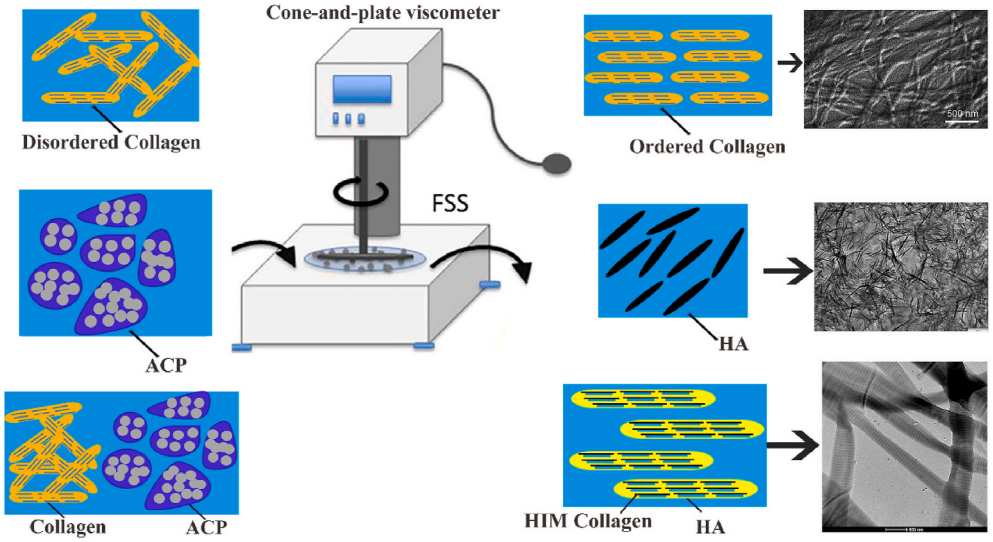

Fig. 9. FSS play an important role in promoting COL mineralization. FSS acting on COL fibers promoted the fibers assemble in single direction to form an ordered structure. Figure from reference 146. FSS acting on ACP promoted its transition to HA. FSS acting on composite solution of COL and ACP formed HIM COL.

research currently. How to apply it to the whole tissue engineering is also a challenge.

3.1.2. Morphology

For a good bone repair scaffold, it also has certain morphological requirements, such as high porosity with a large surface area to volume ratio, sufficient pore size to promote cell seeding and diffusion in the entire structure, Special network shapes with similar natural matrix structure, etc. [149–151]. The MCSs fabricated by different methods exhibited distinct morphologies, which will affect the bone repair performance of scaffold.

The nano-HA directly mixed with COL solution to prepare bio-ink and print the COL/HA scaffold. The calcium ions added into COL solution to print scaffold and then added to the PBS with cross-linkage, so that HA mineralization and COL cross-linking occurred simultaneously. The MCSs fabricated by co-precipitation exhibited more uniformly dispersed nanoparticles and improved homogeneity. Compared with the control group, the biocompatibility and cell adhesion of co-precipitation MCSs is better [152].

Cunniffe et al. [153] fabricated the MCSs by two methods: direct addition of HA method (suspension method) and co-precipitation self--assembly method (immersion method). In the suspension method, HA particles suspended in water added to COL slurry to mix fully, and next freeze-dried to obtain the MCSs (s- MCSs). The immersion method fabricated the MCSs (i- MCSs) by immersing COL scaffold in HA suspension and then freeze-drying. The porosity of MCSs fabricated by two methods both maintained above 98.9%, but there still existed differences in morphology and performance. The mineral content and mechanical properties of s-scaffold was improved compared to i-scaffold. At higher initial calcium and phosphate precursor concentrations, the mineral particles on i-scaffold produced an aggregation effect to obtain larger-sized particles. These larger particles could not penetrate the internal structure of COL fibers during the immersion process.

The morphology of MCSs will affect its performance. Different fabrication methods and materials are the reasons for distinct morphologies. At present, it seems that MCSs fabricated by in-situ precipitation strategy exhibit better like-bone structure than direct addition method. The MCSs with uniformly distributed mineral represented

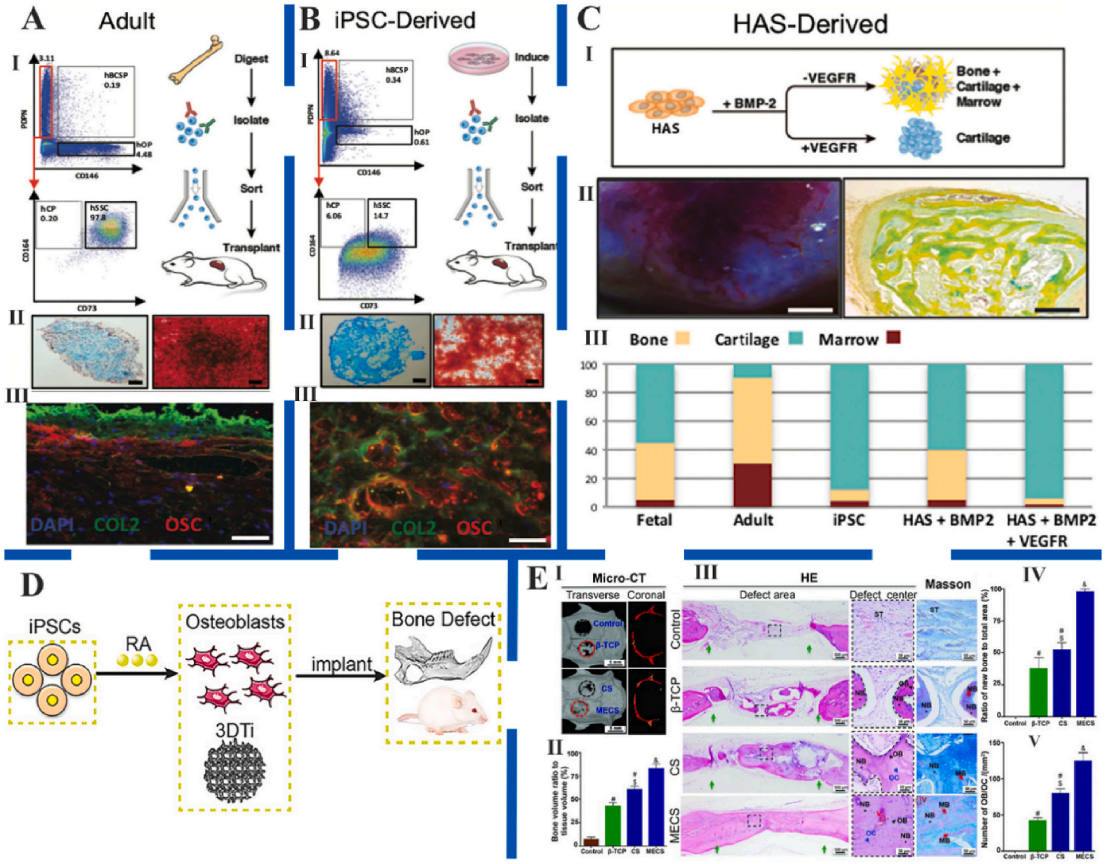

Fig. 10. Different types of stem cells promoted new bone formation. A and B: The human skeletal stem cells (hSSCs) isolated from adult human femur tissue (A) and induction of human monocyte-derived iPSCs (B) promoted osteogenic effect. I) Experimental strategy (right) and representative FACS plots (left) showing gating scheme for isolation of hSSCs from adult human femurhead tissue. II) Alcian blue stain (left) and Alizarin Red stain (right) showing cartilage and bone tissue in a cross-section of micro-mass generated by adult hSSCs after differentiation *in vitro*. Scale bar, 500 μm and 100 μm, respectively. III) IHC staining of cross-section of the ossicle and cartilage for nuclei with DAPI, and bone with anti-collagen II (COL2), and *anti*-osteocalcin (OSC) antibodies, respectively. Scale bar, 100 μm. C: Isolation of hSSCs from BMP2-treated human adipose stroma (B-HAS). I) Experimental strategy for human adipose stroma (HAS) induction with either BMP2 alone or with co-delivery of BMP2 and soluble VEGF receptor (sVEGFR). II) Image (left) and MP stain (right) of vascularized ossicle generated 4 weeks after subcutaneous transplantation of HAS treated with BMP2 in NSG mice. Scale bar, 2 mm and 200 μm, respectively. III) Bar chart showing quantification of percent contribution by the different skeletal fates to total graft mass for grafts derived from fetal hSSCs, adult hSSCs, skeletal-induced-iPSC, B-HAS, or BMP2 + sVEGFR-treated HAS after morphometric analysis. Figure from reference 154. D: The potential mechanism of RA-dependent iPSC osteogenesis. Retinoic acid (RA) bound to retinoic acid receptor (RAR), which further activated the downstream pathway to enhance osteogenic gene expression. Figure from reference 155. E: The stem cell microspheroids (CS) and mineralized ECM/stem cell microspheroids (MECS) promoted bone regeneration in rat calvarial bone defects. I) Representative micro-CT images of CS and MECS post-transplantation in rat calvarial defects at 8 weeks. II) Bone volume analysis based on micro-CT data. III) Hematoxylin and eosin (HE) and Masson staining of the engineered bones. Green arrows represent the bone defect margin. Semi-quantification of new bone (IV) and osteoblasts/osteocytes (V) based on histologic examination. Figure from reference 156.

better bone repair performance than MCSs with aggregated mineral. The mineral ions mineralized in COL fibers to form HIM structure, which is similar to the mineralization process of natural bone.

3.2. Biological cues

3.2.1. Cells as osteogenic promoters

The combination of osteoblasts and MCSs obviously promoted new bone formation effect, but the choice of cells was still a problem that needs to consider. Osteoblasts, mesenchymal stem cells, embryonic stem cells and induced pluripotent stem cells were current choices. Stem cells were the most commonly used in field of bone repair and promoted the osteogenesis of MCSs, as shown in Fig. 10 [154–156]. These cells behaved their specific advantages and shortcomings, so it is necessary to select the most suitable cells for prompting the bone repair effect under different environments.

Osteoblasts were seeded on nanofiber scaffold and monolithic-bulk scaffold and assayed its mineral deposition and osteogenic gene expression. The results showed that nanofiber scaffold exhibited higher osteogenic ability and biomineralization [157,158]. The primary cells as promoters of bone repair scaffold represented obvious effects on osteogenic performance, but there still existed certain problems with this approach [159]. First, the availability of primary cells was limited, and the inherent morbidity of the donor site was not low. Second, the proliferation of primary cells was limited and exhibited age-dependent behavior [160].

Bone marrow stromal cells, also known as mesenchymal stem cells, were often used in bone tissue engineering [161]. Compared with other stem cells, they were harvested relatively easily, and the proliferation rate was faster [162]. At the same time, studies showed that the mesenchymal stem cells seeded on nanofibrous scaffolds can easily differentiate to osteoblasts, so it was the most attractive source of cells for bone tissue engineering [163,164].

Embryonic stem cells were one of the most differentiated stem cell types and exhibited the differentiative ability to almost cell type [165]. It could also be attached on the nanofiber scaffolds and promoted new bone formation, so embryonic stem cells were also a potential option for loading cells on MCSs [166,167]. In addition to the major flaw of limited sources, its moral and political influences were also important factor restricting its application.

Induced pluripotent stem cells and amniotic fluid-derived stem cells were also been proposed as alternatives to embryonic stem cells [168–171]. The two stem cells also exhibited osteogenic differentiation capabilities and played important role in the field of bone repair [172–174]. Whether it produce negatively effect on bone repair process require more experiments to prove.

The osteoblasts and stem cells both play an important role in promoting bone repair [175]. Compared with stem cells, the proliferation and differentiation ability of osteoblasts seeded on scaffolds is insufficient. The stem cells exhibited strong ability of proliferation and differentiation, but there is no consensus of their using conditions. It has great significance for the development of stem cells to establish unified standards and using requirements.

3.2.2. Growth factors

The growth factors mainly include three categories, transforming growth factors (TGF), fibroblast growth factors (FGF) and platelet-derived growth factors (PDGF), in addition to interleukins and other cytokines. The TGF-β produced by bone tissues effectively regulated cell proliferation, differentiation, matrix synthesis, and promoted the ability of chondroblastic and osteoblastic differentiation, which has considerable application in bone repair. Bone morphogenetic proteins (BMPs), as a member of the TGF-β family, exhibited osteoinductive properties [176]. Two of the most frequently used growth factors were BMP-2 and BMP-7, which were available on the market [177]. The recombinant human bone morphogenetic protein 2 (rhBMP-2) represents short retention time and cannot induce bone regeneration after protein failure, so it needs to be sealed in other materials to prolong its release time [178].

The suspensions of chitosan microspheres (CM) were fabricated with rhBMP-2 and then seeded on COL-coated HA scaffold. The HA/COL/CM scaffold obtained by freeze-dried and stored at −20 °C. The release of rhBMP-2 *in vitro* last for more than 21 days and maintained the osteoinductive ability [179]. The HA/COL/CM scaffold achieved localized long-term controlled release of rhBMP-2 and effective bone regeneration ability simultaneously, which provides another research direction for the treatment of bone defects.

The Col-HA/TCP complex filled into distal femoral defect of New Zealand white rabbits and added amount of rhTGF-β1 [180]. When the rhTGF-β1 was not added to bone defect, only small amount of speckled new bone was formed within 15 weeks, and the defect existed fibrous tissue and inflammatory cells. However, when the defect site contained rhTGF-β1, new bone formation was active and obvious mature bone marrow tissue was observed.

The platelet-rich plasma (PRP) was the concentration of autologous plasma platelets and been used in clinical trials. PRP contained various growth factors and cytokines, such as PDGF, TGF-β, FGF and insulin-like growth factor (IGF) [181]. The rhBMP-2 was directly added to COL/PCL-based biphasic calcium phosphate (BCP) scaffold and freeze-dried to obtain COL/PCL-BCP-rhBMP-2 scaffold, as shown in Fig. 11 [182]. In order to fabricate scaffold containing PRP, the COL/PCL-BCP scaffold soaked in PRP solution at 37 °C for 2 h and then freeze-dried. The growth factor added in scaffold exhibited continuously released. The biomineralization scaffold with PRP has higher cell activity and mineral deposition than other scaffolds, which has prompted effect on bone repair.

In addition to TGF, the other two growth factors FGF and PDGF were also prominent in osteogenesis. The composite filler of COL/β-TCP loaded recombinant human fibroblast growth factor 2 (rhFGF-2) significantly promoted bone regeneration at the defect site [183]. The injectable COL powder combined with basic fibroblast growth factor (bFGF) also promoted the repair of bone fractures, and the required protein concentration was low [184]. The COL/β-TCP complex loaded with recombinant human platelet-derived growth factor-BB (rhPDGF-BB) demonstrated excellent biocompatibility, and hPDGF-BB caused bone remodeling and enhanced soft tissue response [185]. The rhPDGF-BB was also added to the injectable collagen/β-TCP matrix, and then used in the senile osteoporosis model of rat. The experimental group containing rhPDGF-BB exhibited a significant enhancement effect on osteogenesis compared with the control group without rhPDGF-BB, and the torsional strength of new bone was equivalent to the contralateral unoperated tibia [186].

The growth factors regulated fracture repair through paracrine or autocrine pathways and exerted a wide range of activities [187]. The tissue engineering scaffold adding growth factors and verifying its role in specific stages of bone healing, which provided direct evidence that growth factors regulate bone repair. It has great significance to combine multiple growth factors in bone repair field [188]. However, limited by intellectual property rights and regulatory approaches, there are few researches on the application of combined growth factors in preclinical or clinical trials, which is also an urgent problem to be solved.

3.3. Chemical cues

3.3.1. Composition differences

According to the composition of natural bone, MCSs as matrix material exhibited a significant effect in promoting bone repair. However, there were still other components in natural bone and the specific role of these components has not been fully understood. Therefore, different or modified materials were added in MCSs to further explore the influence of different components on bone repair performance.

Based on the previous research, Kim et al. [189] further explored the

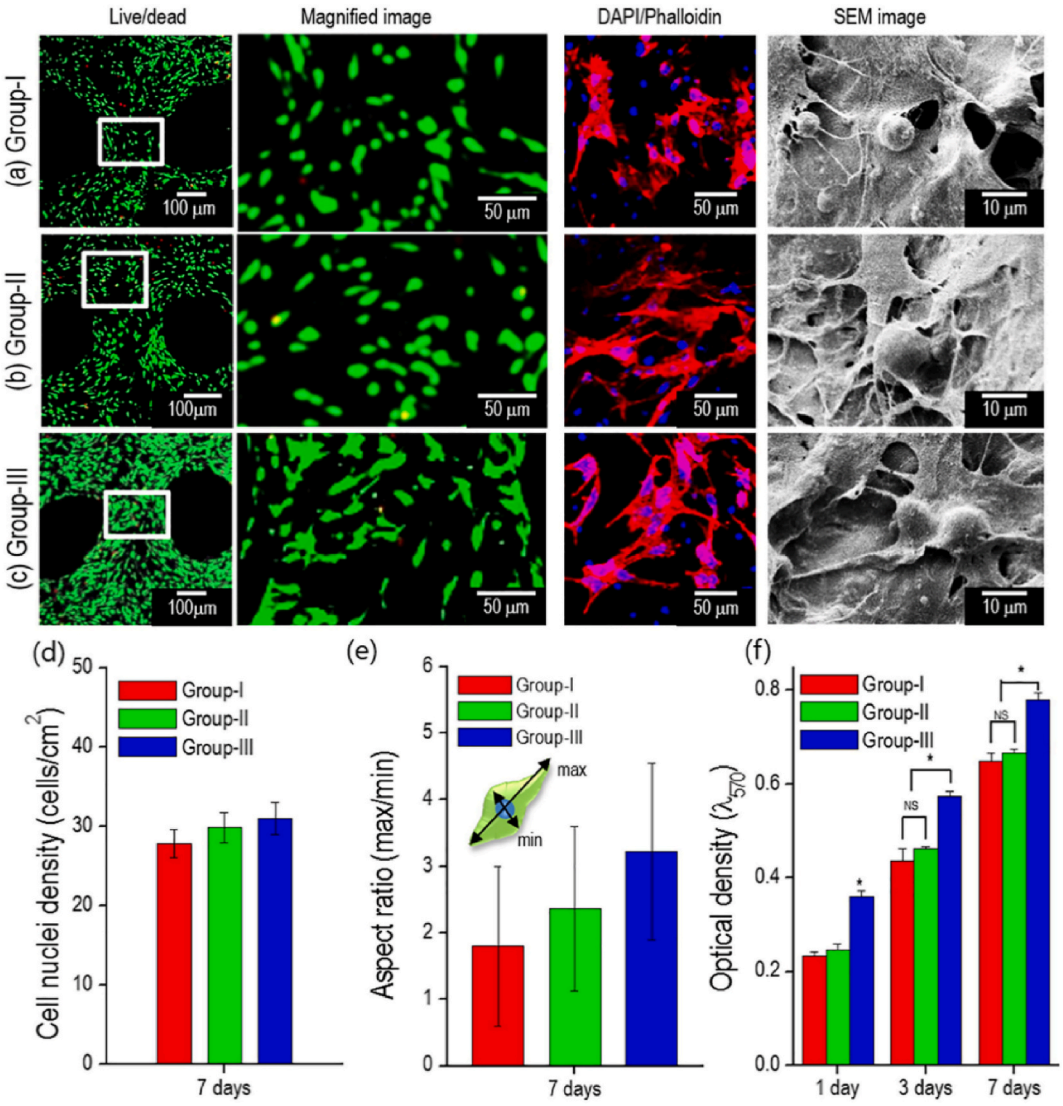

Fig. 11. Morphology and bone repair performance of different groups mineralized scaffold. COL/PCL scaffold embedded with HA/TCP (group-I), HA/TCP/rhBMP-2 (group-II), and HA/TCP/PRP (group-III). Live/dead, DAPI/phalloidin, and SEM images of (a) group-I, (b) group-II, and (c) group-III cultured for 7 days. (d) Number of cells and (e) aspect ratio in the live/dead images. (f) Cell proliferation, as determined by the MTT assay. The asterisks indicate significant differences and "NS" denotes non-significance. Groups II and III promoted the development of cytoskeleton and cell relaxation behavior and induced highly active osteogenic activity. Figure from reference 182.

effect of altered mineral content on the bone repair performance of MCSs. Different amounts of calcium and phosphate ions were added to the COL solution respectively and then mixed the COL solution containing two different mineral ions. The precipitate was collected and freeze-dried to obtain the mineralized COL fiber matrix. The mineralized COL fibrous matrices with different mineral content were dissolved in organic solvents and electrospun to fabricate MCSs. When HA content was 20%, the MCS represented good fiber morphology and mechanical property. However, when mineral content increased to 30%, the fiber morphology was destroyed, and the mechanical property was also affected. At the same time, MC3T3-E1 osteoblasts effectively adhered and actively grew on the MCSs.

The β-TCP was added to COL solution to fabricate the MCSs, which filled the rabbit distal femoral defect as bone void filler and blank filled defect was used as the control group. The addition of β-TCP exhibited positive effect on the mechanical and biological characteristics of scaffold. The high doses of β-TCP nanoparticles caused large amount release of Ca^{2+} ions *in vitro* and better neovascularization *in vivo* [190]. When the mineral content was excessive, it caused excessive Ca^{2+} deposition in bone formation area, which inhibited cell proliferation and restricted the new bone formation.

Since the mineral crystals in natural bone were not a single component, there are some substituents (such as magnesium, carbonate and citrate, etc.). In order to explore the role of different elements in bone formation process, some scholars fabricated modified HA and then combined with COL to form the modified MCSs [191]. Giavaresi [192], Tasciotti [193] and Gulino [194] mixed the magnesium-doped HA (Mg/HA) crystals and COL solution to fabricate MCSs, while He [195] used zinc-doped mesoporous HA microspheres to modify the COL scaffold. Liao et al. [196] fabricated the carbonated nano-HA/COL composite scaffold and found that the crystal morphology changed from plate-like to needle-like and then into spherical particles with increasing carbonate concentration.

In the MCSs, different compositions and mineral contents affected the scaffold performance of bone repair. The interaction of morphology and performance made it difficult to fabricate MCSs that fully composes the natural bone structure. How to balance the function of scaffold morphology and performance was also a major problem in the bone

repair field.

3.3.2. Crosslinking

The triple helix structure of COL exhibited high stability and high degree of self-assembly characteristics. The degree of cross-linking of COL played an important role in stabilizing COL conformation and promoting osteogenesis [197]. There is a major significance to research the role of cross-linking in COL mineralization and reveal effects on the HA deposition [198]. The methods for improving the degree of COL cross-linking were mainly divided into cross-linkage and radiation. The effects of these two cross-linking methods on the MCSs were presented below.

In order to control the mechanical properties and biodegradability of MCSs, glutaraldehyde (GA) as cross-linkage added into the scaffold system. The cross-linkage added to HA/COL suspension and then filtered the precipitate. The cross-linked MCSs obtained by dehydrated and compacted the precipitate. The mechanical properties of scaffold improved with increase of cross-linkage content, but the presence of cross-linkage affected the growth of mineral crystal itself [199]. Animal experiments showed that the scaffold was not toxic, osteoclasts were well absorbed and exhibited good bone conductivity. It indicated that glutaraldehyde as cross-linkage effectively improve the MCSs performance without reducing the biocompatibility of the scaffold, as shown in Fig. 12.

The gamma-ray irradiation possessed the cross-linking effect on COL, which made the pore structure of COL denser without introducing extraneous matter mineralization. The COL irradiated with different doses of gamma-rays and mixed with the mineralized solution with calcium and phosphate ions. The cross-linked MCSs were obtained by freeze-dried precipitate from composite solution. The gamma-ray irradiation not destroyed the COL triple helix structure and made HA attach more on the COL fibers, which improved the mineralization ability of scaffold, as shown in Fig. 12 [200].

The COL cross-linking increased its conformational stability, made the fiber network structure more stable and compact and provided more space for mineral deposition. This cross-linked MCSs provided a potential way to fabricate bone repair materials and the new method for exploring the role of cross-linking in mineralization. The cross-linked MCSs acted *in vivo and in vitro* revealed the effect of cross-linking on HA deposition.

The FSS can simulate the mechanical environment in mineralization process of COL, so it is mostly used for in-situ mineralization methods to fabricate MCSs. The morphology of MCSs mainly depends on the fabrication method, and the appropriate MCSs are fabricated by different methods according to different needs. For example, the nanofiber MCSs fabricated by electrospinning method, the MCSs with regular fiber arrangement fabricated by 3D printing method, and the MCSs containing spherical particles fabricated by vesicle deposition method in situ mineralization. The cells and growth factors promote osteogenesis of MCSs, but the activity of cells and growth factors should be taken up in connection with the fabrication process. At present, the addition of cells and growth factors during the fabrication of MCSs is only possible by 3D printing method. Cross-linking is mainly used in the post-processing of MCSs to improve the mechanical properties and mineralization ability. The different fabrication methods and critical factors in osteogenesis of MCSs can be combined to obtain the best effect.

4. Summary and outlook

In this review, traditional fabrication methods of MCSs were introduced in two ways: direct mineral addition and in-situ mineralization. The minerals and COL in MCSs fabricated by direct mineral addition

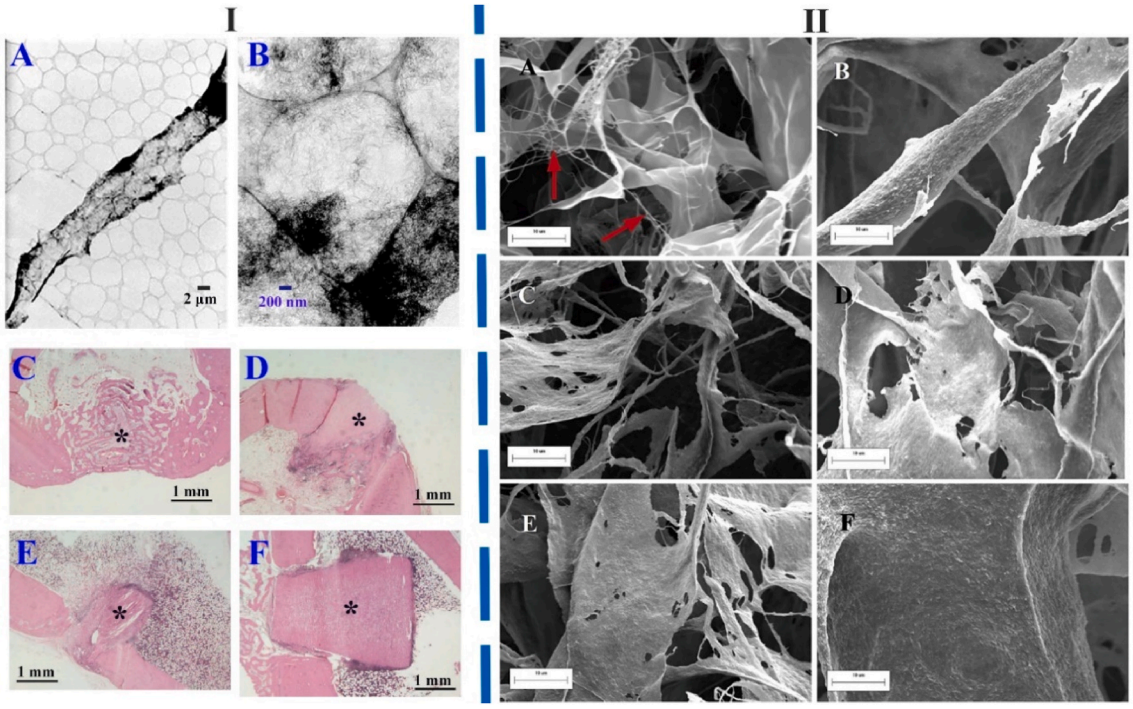

Fig. 12. The morphology of mineralized collagen fabricated by chemical cross-linking (I) and radiation cross-linking (II) methods. I) morphology and bone repair effect of chemical cross-linked mineralized collagen. TEM image of the HA/Col composite cross-linked with GA (A and B). C–F: Bone tissue reactions of the HA/Col composites with serial cross-linkage concentration. C: Non cross-linked (control), D: 0.0191 mmol/gcol, E: 0.191 mmol/gcol, F: 0.675 mmol/gcol and asterisk (*) indicates the HA/Col composite. Neither toxic nor inflammatory reaction was observed. Degradation/resorption with newly bone formation was reduced with increasing GA concentration; however, all composites indicated good bone bonding and osteoconductive properties. Figure from reference 199. II) Morphology of different groups MCSs. A: non-mineralized COL without gamma-ray irradiation. B–F: the mineralized crosslinked COL under gamma-ray irradiation of 0, 2, 4, 6 and 8 KGy dose for 24 h. The fiber surface roughness of MCSs increased, and the interconnected COL microfibers (arrows) decreased significantly compared to the non-MCSs. Figure from reference 200.

were physically compounded. The mineral ions in MCSs fabricated by in-situ mineralization were assembled and crystallized on COL fibers. This is the most significant difference between the two methods. In different reports, the MCSs fabricated by two methods exhibited distinct effects on mechanical and biological properties of bone repair. In accordance with the bionics perspective only, scaffolds fabricated by in-situ mineralization were more structurally similar to natural bones than direct mineral addition.

Moreover, 3D printing as an emerging method for fabrication of MCSs was highlighted. Compared with traditional methods, the most advantage of 3D printing is that can control the fiber arrangement. By controlling microscopic arrangement of scaffold, it possessed the wider applications field. 3D printing as one solution to construct organoids *in vitro*, which solves the problem of how to realize its multi-function. The combination of 3D printing scaffolds with cells and growth factors appears to be a good choice. However, this also put forward higher requirements for the printing inks. In addition to printability such as viscosity, the suitable inks that are conducive to cell growth were also necessary [201]. 3D printing to fabricate multi-functional tissues and organs was the future development direction of regenerative medicine. The MCSs fabricated by 3D printing were treated as an alternative to bone defect or even whole bone. The growth of minerals in COL fibers was a slow process and demanded long time to in-situ mineralization, which is an inevitable problem. The in-situ mineralization in printing COL scaffolds has not been reported yet, and this type bioprinting ink needs further study.

Different fabrication strategies combine COL and minerals to prepare MCSs that are similar to bone tissue in structure, but different MCSs exhibits distinct effects on performance of bone repair. In addition to physical and chemical properties of the MCSs, biological factors such as added cells or growth factors also play an important role. In this paper, we discussed the physical, biological and chemical aspects of MCSs on bone repair performance. The FSS played an important role in orderly COL fiber arrangement and crystal transformation. The morphology of scaffold, such as porosity and fiber diameter, exhibited profound significance for the deposition and proliferation of osteoblasts. Cells and growth factors provided suitable microenvironment for scaffold, which is conducive to the further improvement of osteogenic effect. However, it was not yet conclusive to choose the appropriate cell and growth factor. The COL cross-linking and modified minerals to fabricate scaffolds also have effect on bone repair. The synergy of fabrication method and critical factors in osteogenesis of MCSs makes them exert the better performance of bone repair.

The source of minerals and the control mode of whole mineralization process is also worthy of our concern. Most of the traditional mineral sources are ions or HA crystal. Scholars have proposed to use black phosphorus (BP) as the mineral source to fabricate mineralized scaffold [202]. BP has excellent optical properties, good biocompatibility and biodegradability, so it has captured extensive attention in biomedical applications, such as optical therapy, drug/gene transfer, biological imaging and sensing [203–206]. BP can degrade to produce phosphate in aqueous solution, which can be invoked as a source of phosphate ions. The near infrared (NIR) light promoted the degradation of BP, enhanced the chemical activity of mineral ions and promoted in-situ biomineralization [207,208]. The biomineralization process can be controlled by adjusting the light time and specific location. The BP composite hydrogel scaffolds exhibited a high potential in the mechanical properties and osteoinductive ability in tissue engineering [209]. The selection of mineral source and control of mineralization process also plays an important role in the fabrication of MCSs.

By analyzing these factors, we found that what these researchers want to solve is precisely the difference between MCSs and natural bone. Some challenges still exist when MCSs are used in bone repair and not yet been solved. It can be summarized as the following questions:

1. The research showed that when calcium ion concentration arrives at a certain threshold, it stimulated behavior of osteoblasts [210]. What kind of mineral content of scaffold is the most optimal option in osteogenesis? When the content is too high or low, does it have negative effect on bone repair?
2. Does bone matrix units have the minimum or maximum size? If this critical size exists, can it be used as reference standard for MCSs?
3. The anisotropic characteristics and morphological differences of bone in different parts are not completely understood. How to fabricate the MCSs with different mechanical properties according to natural bone?
4. The bottom-up assembly form of natural bone exhibited excellent mechanical properties. In process of fabricating MCSs, whether two components (CA and HA) can assemble quickly and efficiently as the same way of natural bone?
5. The natural bone contained a variety of minerals, although apatite crystals were absolutely dominant. What roles do the other mineral crystals play in the formation of new bones? Whether the various mineral crystals interact during bone formation process?
6. In addition to the traditional ions and apatite crystals, how to choose more extensive mineral sources? How to realize remote control of fixed-point mineralization *in vitro* through light, heat, electricity and other signals?

If we have a more in-depth understanding of these issues, we may be able to make further research on how to balance the performance and morphology of MCSs. In order to obtain an ideal effect of bone repair, the MCSs fabricates with excellent morphology and performance and provides the microenvironment similar to natural bone matrix. This multi-functional scaffold plays an important role in the field of bone repair and diseases, which also affected in the micro level, such as osteoporosis, osteoarthritis and other degenerative diseases.

CRediT authorship contribution statement

Zhengwei Li: Investigation, Data curation, Writing - original draft. **Tianming Du:** Resources. **Changshun Ruan:** Conceptualization, Supervision, Writing - review & editing. **Xufeng Niu:** Conceptualization, Supervision, Writing - review & editing.

Declaration of competing interest

None.

Acknowledgement

The authors gratefully acknowledge the support for this work from the National Key Research and Development Program of China [Grant No. 2018YFA0703100]; the National Natural Science Foundation of China [Grant Nos.11872097, 82072082]; the Youth Innovation Promotion Association of CAS [Grant No. 2019350]; Beijing Natural Science Foundation [No. L182017]; the 111 Project [No. B13003] and the Shenzhen Fundamental Research Foundation [Grant No. JCYJ20180507182237428].

References

[1] T. Hassenkam, G.E. Fantner, J.A. Cutroni, J.C. Weaver, D.E. Morse, P.K. Hansma, High-resolution AFM imaging of intact and fractured trabecular bone, Bone 35 (2004) 4–10, https://doi.org/10.1016/j.bone.2004.02.024.
[2] T.A. Taton, Nanotechnology - boning up on biology, Nature 412 (2001) 491–492, https://doi.org/10.1038/35087687.
[3] J.S. Yerramshetty, O. Akkus, The associations between mineral crystallinity and the mechanical properties of human cortical bone, Bone 42 (2008) 476–482, https://doi.org/10.1016/j.bone.2007.12.001.
[4] J.J. Kruzic, R.O. Ritchie, Fatigue of mineralized tissues: cortical bone and dentin, J Mech Behav Biomed Mater 1 (2008) 3–17, https://doi.org/10.1016/j.jmbbm.2007.04.002.

[5] O. Akkus, F. Adar, M.B. Schaffler, Age-related changes in physicochemical properties of mineral crystals are related to impaired mechanical function of cortical bone, Bone 34 (2004) 443–453, https://doi.org/10.1016/j.bone.2003.11.003.

[6] W.T. George, D. Vashishth, Susceptibility of aging human bone to mixed-mode fracture increases bone fragility, Bone 38 (2006) 105–111, https://doi.org/10.1016/j.bone.2005.08.002.

[7] S.P. Kotha, N. Guzelsu, Tensile damage and its effects on cortical bone, J. Biomech. 36 (2003) 1683–1689, https://doi.org/10.1016/s0021-9290(03)00169-6.

[8] J.D.J. Black, B.J. Tadros, Bone structure: from cortical to calcium, J. Orthop. Traumatol. 34 (2020) 113–119, https://doi.org/10.1016/j.mporth.2020.03.002.

[9] B.L. Smith, T.E. Schaeffer, M. Viani, J.B. Thompson, N.A. Frederick, J. Kindt, A. Belcher, G.D. Stucky, D.E. Morse, P.K. Hansma, Molecular mechanistic origin of the toughness of natural adhesives, fibres and composites, Nature 399 (1999) 761–763, https://doi.org/10.1038/21607.

[10] D.B. Burr, The contribution of the organic matrix to bone's material properties, Bone 31 (2002) 8–11, https://doi.org/10.1016/s8756-3282(02)00815-3.

[11] G.E. Fantner, T. Hassenkam, J.H. Kindt, J.C. Weaver, H. Birkedal, L. Pechenik, J. A. Cutroni, G.A. Cidade, G.D. Stucky, D.E. Morse, P.K. Hansma, Sacrificial bonds and hidden length dissipate energy as mineralized fibrils separate during bone fracture, Nat. Mater. 4 (2005) 612–616, https://doi.org/10.1038/nmat1428.

[12] X.F. Niu, R. Fan, F. Tian, X.L. Guo, P. Li, Q.L. Feng, Y.B. Fan, Calcium concentration dependent collagen mineralization, Mater. Sci. Eng. C 73 (2017) 137–143, https://doi.org/10.1016/j.msec.2016.12.079.

[13] E. Beniash, Biominerals–hierarchical nanocomposites: the example of bone, Wiley Interdiscip Rev Nanomed Nanobiotechnol. 3 (2011) 47–69, https://doi.org/10.1002/wnan.105.

[14] P. Fratzl, R. Weinkamer, Nature's hierarchical materials, Prog. Mater. Sci. 52 (2007) 1263–1334, https://doi.org/10.1016/j.pmatsci.2007.06.001.

[15] C.T. Thorpe, I. Streeter, G.L. Pinchbeck, A.E. Goodship, P.D. Clegg, H.L. Birch, Aspartic acid racemization and collagen degradation markers reveal an accumulation of damage in tendon collagen that is enhanced with aging, J. Biol. Chem. 285 (2010) 15674–15681, https://doi.org/10.1074/jbc.M109.077503.

[16] J. Orgel, T.C. Irving, A. Miller, T.J. Wess, Microfibrillar structure of type I collagen in situ, Proc. Natl. Acad. Sci. U.S.A. 103 (2006) 9001–9005, https://doi.org/10.1073/pnas.0502718103.

[17] X. Niu, Q. Feng, M. Wang, X. Guo, Q. Zheng, Porous nano-HA/collagen/PLLA scaffold containing chitosan microspheres for controlled delivery of synthetic peptide derived from BMP-2, J. Contr. Release 134 (2009) 111–117, https://doi.org/10.1016/j.jconrel.2008.11.020.

[18] E. Davies, K.H. Muller, W.C. Wong, C.J. Pickard, D.G. Reid, J.N. Skepper, M. J. Duer, Citrate bridges between mineral platelets in bone, Proc. Natl. Acad. Sci. U.S.A. 111 (2014) E1354–E1363, https://doi.org/10.1073/pnas.1315080111.

[19] E. Bonucci, Bone mineralization, Front. Biosci. 17 (2012) 100–128, 10.2741/3918.

[20] A. George, A. Veis, Phosphorylated proteins and control over apatite nucleation, crystal growth, and inhibition, Chem. Rev. 108 (2008) 4670–4693, https://doi.org/10.1021/cr0782729.

[21] K. Chatzipanagis, M. Iafisco, T. Roncal-Herrero, M. Bilton, A. Tampieri, R. Kröger, J.M. Delgado-López, Crystallization of citrate-stabilized amorphous calcium phosphate to nanocrystalline apatite: a surface-mediated transformation, CrystEngComm 18 (2016) 3170–3173, https://doi.org/10.1039/c6ce00521g.

[22] D.J. Huey, K.A. Athanasiou, Tension-compression loading with chemical stimulation results in additive increases to functional properties of anatomic meniscal constructs, PloS One 6 (2011), e27857, https://doi.org/10.1371/journal.pone.0027857.

[23] L. Yang, C.F.C. Fitié, K.O. van der Werf, M.L. Bennink, P.J. Dijkstra, J. Feijen, Mechanical properties of single electrospun collagen type I fibers, Biomaterials 29 (2008) 955–962, https://doi.org/10.1016/j.biomaterials.2007.10.058.

[24] Y.-K. Seo, H.-H. Youn, C.-S. Park, K.-Y. Song, J.-K. Park, Reinforced bioartificial dermis constructed with collagen threads, Biotechnol. Bioproc. Eng. 13 (2009) 745–751, https://doi.org/10.1007/s12257-008-0118-0.

[25] P. Miranda, A. Pajares, E. Saiz, A.P. Tomsia, F. Guiberteau, Fracture modes under uniaxial compression in hydroxyapatite scaffolds fabricated by robocasting, J. Biomed. Mater. Res. 83 (2007) 646–655, https://doi.org/10.1002/jbm.a.31272.

[26] E. Charriere, J. Lemaitre, P. Zysset, Hydroxyapatite cement scaffolds with controlled macroporosity: fabrication protocol and mechanical properties, Biomaterials 24 (2003) 809–817, https://doi.org/10.1016/s0142-9612(02)00406-4.

[27] J.M. Cordell, M.L. Vogl, A.J. Wagoner Johnson, The influence of micropore size on the mechanical properties of bulk hydroxyapatite and hydroxyapatite scaffolds, J Mech Behav Biomed Mater 2 (2009) 560–570, https://doi.org/10.1016/j.jmbbm.2009.01.009.

[28] D.T. Reilly, A.H. Burstein, The elastic and ultimate properties of compact bone tissue, J. Biomech. 8 (1975) 393–405, https://doi.org/10.1016/0021-9290(75)90075-5.

[29] R. Belda, M. Palomar, J.L. Peris-Serra, A. Vercher-Martínez, E. Giner, Compression failure characterization of cancellous bone combining experimental testing, digital image correlation and finite element modeling, Int. J. Mech. Sci. 165 (2020), 105213, https://doi.org/10.1016/j.ijmecsci.2019.105213.

[30] K. Bruyere Garnier, R. Dumas, C. Rumelhart, M.E. Arlot, Mechanical characterization in shear of human femoral cancellous bone: torsion and shear tests, Med. Eng. Phys. 21 (1999) 641–649, https://doi.org/10.1016/s1350-4533(99)00096-x.

[31] M. Halawa, A.J. Lee, R.S. Ling, S.S. Vangala, The shear strength of trabecular bone from the femur, and some factors affecting the shear strength of the cement-bone interface, Archives of orthopaedic and traumatic surgery, Archiv fur orthopadische und Unfall-Chirurgie. 92 (1978) 19–30, https://doi.org/10.1007/bf00381636.

[32] A. Nazarian, D. Meier, R. Muller, B.D. Snyder, Functional dependence of cancellous bone shear properties on trabecular microstructure evaluated using time-lapsed micro-computed tomographic imaging and torsion testing, J. Orthop. Res. 27 (2009) 1667–1674, https://doi.org/10.1002/jor.20931.

[33] A. Kaminski, A. Jastrzebska, E. Grazka, J. Marowska, G. Gut, A. Wojciechowski, I. Uhrynowska-Tyszkiewicz, Effect of gamma irradiation on mechanical properties of human cortical bone: influence of different processing methods, Cell Tissue Bank. 13 (2012) 363–374, https://doi.org/10.1007/s10561-012-9308-2.

[34] A. Kaminski, E. Grazka, A. Jastrzebska, J. Marowska, G. Gut, A. Wojciechowski, I. Uhrynowska-Tyszkiewicz, Effect of accelerated electron beam on mechanical properties of human cortical bone: influence of different processing methods, Cell Tissue Bank. 13 (2012) 375–386, https://doi.org/10.1007/s10561-012-9312-6.

[35] S. Haimi, A. Vienonen, M. Hirn, M. Pelto, V. Virtanen, R. Suuronen, The effect of chemical cleansing procedures combined with peracetic acid-ethanol sterilization on biomechanical properties of cortical bone, Biologicals 36 (2008) 99–104, https://doi.org/10.1016/j.biologicals.2007.06.001.

[36] J.B. Thompson, J.H. Kindt, B. Drake, H.G. Hansma, D.E. Morse, P.K. Hansma, Bone indentation recovery time correlates with bond reforming time, Nature 414 (2001) 773–776, https://doi.org/10.1038/414773a.

[37] S. Weiner, H.D. Wagner, The material bone: structure mechanical function relations, Annu. Rev. Mater. Sci. 28 (1998) 271–298, https://doi.org/10.1146/annurev.matsci.28.1.271.

[38] N. Reznikov, R. Shahar, S. Weiner, Bone hierarchical structure in three dimensions, Acta Biomater. 10 (2014) 3815–3826, https://doi.org/10.1016/j.actbio.2014.05.024.

[39] N. Reznikov, M. Bilton, L. Lari, M.M. Stevens, R. Kroger, Fractal-like hierarchical organization of bone begins at the nanoscale, Science 360 (2018), eaao2189, https://doi.org/10.1126/science.aao2189.

[40] I. Jager, P. Fratzl, Mineralized collagen fibrils: a mechanical model with a staggered arrangement of mineral particles, Biophys. J. 79 (2000) 1737–1746, https://doi.org/10.1016/s0006-3495(00)76426-5.

[41] F. Nudelman, K. Pieterse, A. George, P.H. Bomans, H. Friedrich, L.J. Brylka, P. A. Hilbers, G. de With, N.A. Sommerdijk, The role of collagen in bone apatite formation in the presence of hydroxyapatite nucleation inhibitors, Nat. Mater. 9 (2010) 1004–1009, https://doi.org/10.1038/nmat2875.

[42] H.P. Schwarcz, D.M. Binkley, L. Luo, K. Grandfield, A search for apatite crystals in the gap zone of collagen fibrils in bone using dark-field illumination, Bone 135 (2020), 115304, https://doi.org/10.1016/j.bone.2020.115304.

[43] D.R. Katti, S.M. Pradhan, K.S. Katti, Directional dependence of hydroxyapatite-collagen interactions on mechanics of collagen, J. Biomech. 43 (2010) 1723–1730, https://doi.org/10.1016/j.jbiomech.2010.02.027.

[44] F.C. Fierz, F. Beckmann, M. Huser, S.H. Irsen, B. Leukers, F. Witte, O. Degistirici, A. Andronache, M. Thie, B. Muller, The morphology of anisotropic 3D-printed hydroxyapatite scaffolds, Biomaterials 29 (2008) 3799–3806, https://doi.org/10.1016/j.biomaterials.2008.06.012.

[45] V.I. Shubayev, R. Branemark, J. Steinauer, R.R. Myers, Titanium implants induce expression of matrix metalloproteinases in bone during osseointegration, J. Rehabil. Res. Dev. 41 (2004) 757–765, https://doi.org/10.1682/jrrd.2003.07.0107.

[46] M. Schlumberger, R. Mayr, C. Koidl, M. Eichinger, T. Roth, Treatment of tibial nonunion with bone defect using a heterotopic ossification as autologous bone graft: literature overview and case report, Eur. J. Orthop. Surg. Traumatol. 28 (2018) 741–746, https://doi.org/10.1007/s00590-018-2146-6.

[47] J.M. Holzwarth, P.X. Ma, Biomimetic nanofibrous scaffolds for bone tissue engineering, Biomaterials 32 (2011) 9622–9629, https://doi.org/10.1016/j.biomaterials.2011.09.009.

[48] M. Di Monaco, F. Vallero, R. Di Monaco, R. Tappero, A. Cavanna, Fat mass and skeletal muscle mass in hip-fracture women: a cross-sectional study, Maturitas 56 (2007) 404–410, https://doi.org/10.1016/j.maturitas.2006.11.003.

[49] W.H. Wang, K.W.K. Yeung, Bone grafts and biomaterials substitutes for bone defect repair: a review, Bioact Mater 2 (2017) 224–247, https://doi.org/10.1016/j.bioactmat.2017.05.007.

[50] P.V. Mummaneni, G. Rodts, R. Haid, H. Deutsch, The decision-making process: allograft versus autograft, Neurosurgery 60 (2007) 98–102, https://doi.org/10.1227/01.neu.0000249221.50085.ad.

[51] Z.S. Haidar, R.C. Hamdy, M. Tabrizian, Delivery of recombinant bone morphogenetic proteins for bone regeneration and repair. Part A: current challenges in BMP delivery, Biotechnol. Lett. 31 (2009) 1817–1824, https://doi.org/10.1007/s10529-009-0099-x.

[52] H. Qu, H. Fu, Z. Han, Y. Sun, Biomaterials for bone tissue engineering scaffolds: a review, RSC Adv. 9 (2019) 26252–26262, https://doi.org/10.1039/c9ra05214c.

[53] Y.Z. Cai, L.L. Wang, H.X. Cai, Y.Y. Qi, X.H. Zou, H.W. Ouyang, Electrospun nanofibrous matrix improves the regeneration of dense cortical bone, J. Biomed. Mater. Res. 95 (2010) 49–57, https://doi.org/10.1002/jbm.a.32816.

[54] B. Leukers, H. Gulkan, S.H. Irsen, S. Milz, C. Tille, M. Schieker, H. Seitz, Hydroxyapatite scaffolds for bone tissue engineering made by 3D printing, J. Mater. Sci. Mater. Med. 16 (2005) 1121–1124, https://doi.org/10.1007/s10856-005-4716-5.

[55] J. Bramhill, S. Ross, G. Ross, Bioactive nanocomposites for tissue repair and regeneration: a review, Int. J. Environ. Res. Publ. Health 14 (2017), https://doi.org/10.3390/ijerph14010066.

[56] L. Li, H. Lu, Y. Zhao, J. Luo, L. Yang, W. Liu, Q. He, Functionalized cell-free scaffolds for bone defect repair inspired by self-healing of bone fractures: a review and new perspectives, Mater. Sci. Eng. C 98 (2019) 1241–1251, https://doi.org/10.1016/j.msec.2019.01.075.
[57] F. Yang, X. Niu, X. Gu, C. Xu, W. Wang, Y. Fan, Biodegradable magnesium-incorporated poly(l-lactic acid) microspheres for manipulation of drug release and alleviation of inflammatory response, ACS Appl. Mater. Interfaces 11 (2019) 23546–23557, https://doi.org/10.1021/acsami.9b03766.
[58] G. Turnbull, J. Clarke, F. Picard, P. Riches, L.L. Jia, F.X. Han, B. Li, W.M. Shu, 3D bioactive composite scaffolds for bone tissue engineering, Bioact Mater 3 (2018) 278–314, https://doi.org/10.1016/j.bioactmat.2017.10.001.
[59] D.B. Raina, I. Qayoom, D. Larsson, M.H. Zheng, A. Kumar, H. Isaksson, L. Lidgren, M. Tagil, Guided tissue engineering for healing of cancellous and cortical bone using a combination of biomaterial based scaffolding and local bone active molecule delivery, Biomaterials 188 (2019) 38–49, https://doi.org/10.1016/j.biomaterials.2018.10.004.
[60] D. Lin, Y.J. Chai, Y.F. Ma, B. Duan, Y. Yuan, C.S. Liu, Rapid initiation of guided bone regeneration driven by spatiotemporal delivery of IL-8 and BMP-2 from hierarchical MBG-based scaffold, Biomaterials 196 (2019) 122–137, https://doi.org/10.1016/j.biomaterials.2017.11.011.
[61] R. Florencio-Silva, G.R. Sasso, E. Sasso-Cerri, M.J. Simoes, P.S. Cerri, Biology of bone tissue: structure, function, and factors that influence bone cells, BioMed Res. Int. 2015 (2015) 421746, https://doi.org/10.1155/2015/421746.
[62] L.L. Hench, I. Thompson, Twenty-first century challenges for biomaterials, J. R. Soc. Interface 7 (2010) 379–391, https://doi.org/10.1098/rsif.2010.0151.focus.
[63] H.L. Oliveira, W.L.O. Da Rosa, C.E. Cuevas-Suarez, N.L.V. Carreno, A.F. da Silva, T.N. Guim, O.A. Dellagostin, E. Piva, Histological evaluation of bone repair with hydroxyapatite: a systematic review, Calcif. Tissue Int. 101 (2017) 341–354, https://doi.org/10.1007/s00223-017-0294-z.
[64] C. Gao, D. Wei, H. Yang, T. Chen, L. Yang, Nanotechnology for treating osteoporotic vertebral fractures, Int. J. Nanomed. 10 (2015) 5139–5157. http://doi.org/10.2147/IJN.S85037.
[65] M. Jayabalan, K.T. Shalumon, M.K. Mitha, K. Ganesan, M. Epple, Effect of hydroxyapatite on the biodegradation and biomechanical stability of polyester nanocomposites for orthopaedic applications, Acta Biomater. 6 (2010) 763–775, https://doi.org/10.1016/j.actbio.2009.09.015.
[66] K. Tuzlakoglu, M.I. Santos, N. Neves, R.L. Reis, Design of nano- and microfiber combined scaffolds by electrospinning of collagen onto starch-based fiber meshes: a man-made equivalent of natural extracellular matrix, Tissue Eng. 17 (2011) 463–473, https://doi.org/10.1089/ten.TEA.2010.0178.
[67] S. Kuttappan, D. Mathew, M.B. Nair, Biomimetic composite scaffolds containing bioceramics and collagen/gelatin for bone tissue engineering - a mini review, Int. J. Biol. Macromol. 93 (2016) 1390–1401, https://doi.org/10.1016/j.ijbiomac.2016.06.043.
[68] A. Oryan, S. Alidadi, A. Moshiri, N. Maffulli, Bone regenerative medicine: classic options, novel strategies, and future directions, J. Orthop. Surg. Res. 9 (2014) 27, https://doi.org/10.1186/1749-799x-9-18.
[69] D.H. Reneker, A.L. Yarin, Electrospinning jets and polymer nanofibers, Polymer 49 (2008) 2387–2425, https://doi.org/10.1016/j.polymer.2008.02.002.
[70] A. Greiner, J.H. Wendorff, Electrospinning: a fascinating method for the preparation of ultrathin fibers, Angew Chem. Int. Ed. Engl. 46 (2007) 5670–5703, https://doi.org/10.1002/anie.200604646.
[71] H. Peng, Z. Yin, H. Liu, X. Chen, B. Feng, H. Yuan, B. Su, H. Ouyang, Y. Zhang, Electrospun biomimetic scaffold of hydroxyapatite/chitosan supports enhanced osteogenic differentiation of mMSCs, Nanotechnology 23 (2012), 485102, https://doi.org/10.1088/0957-4484/23/48/485102.
[72] Y.Z. Zhang, J.R. Venugopal, A. El-Turki, S. Ramakrishna, B. Su, C.T. Lim, Electrospun biomimetic nanocomposite nanofibers of hydroxyapatite/chitosan for bone tissue engineering, Biomaterials 29 (2008) 4314–4322, https://doi.org/10.1016/j.biomaterials.2008.07.038.
[73] S. Jin, F. Sun, Q. Zou, J. Huang, Y. Zuo, Y. Li, S. Wang, L. Cheng, Y. Man, F. Yang, J. Li, Fish collagen and hydroxyapatite reinforced poly(lactide- co-glycolide) fibrous membrane for guided bone regeneration, Biomacromolecules 20 (2019) 2058–2067, https://doi.org/10.1021/acs.biomac.9b00267.
[74] M.P. Prabhakaran, J. Venugopal, S. Ramakrishna, Electrospun nanostructured scaffolds for bone tissue engineering, Acta Biomater. 5 (2009) 2884–2893, https://doi.org/10.1016/j.actbio.2009.05.007.
[75] J. Venugopal, P. Vadgama, T.S.S. Kumar, S. Ramakrishna, Biocomposite nanofibres and osteoblasts for bone tissue engineering, Nanotechnology 18 (2007), 055101, https://doi.org/10.1088/0957-4484/18/5/055101.
[76] J. Venugopal, S. Low, A.T. Choon, T.S. Sampath Kumar, S. Ramakrishna, Mineralization of osteoblasts with electrospun collagen/hydroxyapatite nanofibers, J. Mater. Sci. Mater. Med. 19 (2008) 2039–2046, https://doi.org/10.1007/s10856-007-3289-x.
[77] J.R. Venugopal, S. Low, A.T. Choon, A.B. Kumar, S. Ramakrishna, Nanobioengineered electrospun composite nanofibers and osteoblasts for bone regeneration, Artif. Organs 32 (2008) 388–397, https://doi.org/10.1111/j.1525-1594.2008.00557.x.
[78] J. Venugopal, S. Low, A.T. Choon, S. Ramakrishna, Interaction of cells and nanofiber scaffolds in tissue engineering, J. Biomed. Mater. Res. B 84 (2008) 34–48, https://doi.org/10.1002/jbm.b.30841.
[79] J. Venugopal, M.P. Prabhakaran, S. Low, A.T. Choon, Y.Z. Zhang, G. Deepika, S. Ramakrishna, Nanotechnology for nanomedicine and delivery of drugs, Curr. Pharmaceut. Des. 14 (2008) 2184–2200, https://doi.org/10.2174/138161208785740180.
[80] D.A. Wahl, J.T. Czernuszka, Collagen-hydroxyapatite composites for hard tissue repair, Eur. Cell. Mater. 11 (2006) 43–56, https://doi.org/10.22203/ecm.v011a06.
[81] G.M. Cunniffe, C.M. Curtin, E.M. Thompson, G.R. Dickson, F.J. O'Brien, Content-dependent osteogenic response of nanohydroxyapatite: an in vitro and in vivo assessment within collagen-based scaffolds, ACS Appl. Mater. Interfaces 8 (2016) 23477–23488, https://doi.org/10.1021/acsami.6b06596.
[82] H. Tebyanian, M.H. Norahan, H. Eyni, M. Movahedin, S.J. Mortazavi, A. Karami, M.R. Nourani, N. Baheiraei, Effects of collagen/beta-tricalcium phosphate bone graft to regenerate bone in critically sized rabbit calvarial defects, J. Appl. Biomater. Funct. Mater. 17 (2019), 2280800018820490, http://doi.org/10.1177/2280800018820490.
[83] D.A. Wahl, E. Sachlos, C. Liu, J.T. Czernuszka, Controlling the processing of collagen-hydroxyapatite scaffolds for bone tissue engineering, J. Mater. Sci. Mater. Med. 18 (2007) 201–209, https://doi.org/10.1007/s10856-006-0682-9.
[84] E. Andronescu, G. Voicu, M. Ficai, I.A. Mohora, R. Trusca, A. Ficai, Collagen/hydroxyapatite composite materials with desired ceramic properties, J. Electron. Microsc. 60 (2011) 253–259, https://doi.org/10.1093/jmicro/dfr010.
[85] J. He, T. Huang, L. Gan, Z. Zhou, B. Jiang, Y. Wu, F. Wu, Z. Gu, Collagen-infiltrated porous hydroxyapatite coating and its osteogenic properties: in vitro and in vivo study, J. Biomed. Mater. Res. 100 (2012) 1706–1715, https://doi.org/10.1002/jbm.a.34121.
[86] H. Melero, N. Garcia-Giralt, J. Fernández, A. Díez-Pérez, J.M. Guilemany, Comparison of in vitro behavior of as-sprayed, alkaline-treated and collagen-treated bioceramic coatings obtained by high velocity oxy-fuel spray, Appl. Surf. Sci. 307 (2014) 246–254, https://doi.org/10.1016/j.apsusc.2014.04.021.
[87] G.M. Whitesides, B. Grzybowski, Self-assembly at all scales, Science 295 (2002) 2418–2421, https://doi.org/10.1126/science.1070821.
[88] Y. Liu, N. Li, Y.P. Qi, L. Dai, T.E. Bryan, J. Mao, D.H. Pashley, F.R. Tay, Intrafibrillar collagen mineralization produced by biomimetic hierarchical nanoapatite assembly, Adv. Mater. 23 (2011) 975–980, https://doi.org/10.1002/adma.201003882.
[89] C. Hu, M. Zilm, M. Wei, Fabrication of intrafibrillar and extrafibrillar mineralized collagen/apatite scaffolds with a hierarchical structure, J. Biomed. Mater. Res. 104 (2016) 1153–1161, https://doi.org/10.1002/jbm.a.35649.
[90] Y. Liu, Y.K. Kim, L. Dai, N. Li, S.O. Khan, D.H. Pashley, F.R. Tay, Hierarchical and non-hierarchical mineralisation of collagen, Biomaterials 32 (2011) 1291–1300, https://doi.org/10.1016/j.biomaterials.2010.10.018.
[91] Y. Liu, S. Liu, D. Luo, Z. Xue, X. Yang, L. Gu, Y. Zhou, T. Wang, Hierarchically staggered nanostructure of mineralized collagen as a bone-grafting scaffold, Adv. Mater. 28 (2016) 8740–8748, https://doi.org/10.1002/adma.201602628.
[92] W. Zhang, S.S. Liao, F.Z. Cui, Hierarchical self-assembly of nano-fibrils in mineralized collagen, Chem. Mater. 15 (2003) 3221–3226, https://doi.org/10.1021/cm030080g.
[93] W. Zhang, Z.L. Huang, S.S. Liao, F.Z. Cui, Nucleation sites of calcium phosphate crystals during collagen mineralization, J. Am. Ceram. Soc. 86 (2003) 1052–1054, https://doi.org/10.1111/j.1151-2916.2003.tb03422.x.
[94] F.-Z. Cui, Y. Li, J. Ge, Self-assembly of mineralized collagen composites, Mater. Sci. Eng. R Rep. 57 (2007) 1–27, https://doi.org/10.1016/j.mser.2007.04.001.
[95] C. Du, F.Z. Cui, Q.L. Feng, X.D. Zhu, K. de Groot, Tissue response to nano-hydroxyapatite/collagen composite implants in marrow cavity, J. Biomed. Mater. Res. 42 (1998) 540–548, https://doi.org/10.1002/(sici)1097-4636(19981215)42:4%3C540::aid-jbm9%3E3.0.co;2-2.
[96] H. Liu, M. Lin, X. Liu, Y. Zhang, Y. Luo, Y. Pang, H. Chen, D. Zhu, X. Zhong, S. Ma, Y. Zhao, Q. Yang, X. Zhang, Doping bioactive elements into a collagen scaffold based on synchronous self-assembly/mineralization for bone tissue engineering, Bioact Mater 5 (2020) 844–858, https://doi.org/10.1016/j.bioactmat.2020.06.005.
[97] L.N. Niu, S.E. Jee, K. Jiao, L. Tonggu, M. Li, L. Wang, Y.D. Yang, J.H. Bian, L. Breschi, S.S. Jang, J.H. Chen, D.H. Pashley, F.R. Tay, Collagen intrafibrillar mineralization as a result of the balance between osmotic equilibrium and electroneutrality, Nat. Mater. 16 (2017) 370–378, https://doi.org/10.1038/nmat4789.
[98] Y. Su, I. Cockerill, Y. Zheng, L. Tang, Y.X. Qin, D. Zhu, Biofunctionalization of metallic implants by calcium phosphate coatings, Bioact Mater 4 (2019) 196–206, https://doi.org/10.1016/j.bioactmat.2019.05.001.
[99] S. Bakhshandeh, S. Amin Yavari, Electrophoretic deposition: a versatile tool against biomaterial associated infections, J. Mater. Chem. B 6 (2018) 1128–1148, https://doi.org/10.1039/c7tb02445b.
[100] S. Cometa, M.A. Bonifacio, A.M. Ferreira, P. Gentile, E. De Giglio, Surface characterization of electro-assisted titanium implants: a multi-technique approach, Materials 13 (2020) 705. http://doi.org/10.3390/ma13030705.
[101] R.I. Asri, W.S. Harun, M.A. Hassan, S.A. Ghani, Z. Buyong, A review of hydroxyapatite-based coating techniques: sol-gel and electrochemical depositions on biocompatible metals, J Mech Behav Biomed Mater 57 (2016) 95–108, https://doi.org/10.1016/j.jmbbm.2015.11.031.
[102] S. Manara, F. Paolucci, B. Palazzo, M. Marcaccio, E. Foresti, G. Tosi, S. Sabbatini, P. Sabatino, G. Altankov, N. Roveri, Electrochemically-assisted deposition of biomimetic hydroxyapatite–collagen coatings on titanium plate, Inorg. Chim. Acta. 361 (2008) 1634–1645, https://doi.org/10.1016/j.ica.2007.03.044.
[103] X. Zhao, T. Hu, H. Li, M. Chen, S. Cao, L. Zhang, X. Hou, Electrochemically assisted co-deposition of calcium phosphate/collagen coatings on carbon/carbon composites, Appl. Surf. Sci. 257 (2011) 3612–3619, https://doi.org/10.1016/j.apsusc.2010.11.088.
[104] K. Hoshi, H. Ozawa, Matrix vesicle calcification in bones of adult rats, Calcif. Tissue Int. 66 (2000) 430–434, https://doi.org/10.1007/s002230010087.

[105] Y. Wei, M. Shi, J. Zhang, X. Zhang, K. Shen, R. Wang, R.J. Miron, Y. Xiao, Y. Zhang, Autologous versatile vesicles-incorporated biomimetic extracellular matrix induces biomineralization, Adv. Funct. Mater. (2020), 2000015, https://doi.org/10.1002/adfm.202000015.
[106] A. Pederson, Thermal assembly of a biomimetic mineral/collagen composite, Biomaterials 24 (2003) 4881–4890, https://doi.org/10.1016/s0142-9612(03)00369-7.
[107] C. Dhand, S.T. Ong, N. Dwivedi, S.M. Diaz, J.R. Venugopal, B. Navaneethan, M. Fazil, S.P. Liu, V. Seitz, E. Wintermantel, R.W. Beuerman, S. Ramakrishna, N. K. Verma, R. Lakshminarayanan, Bio-inspired in situ crosslinking and mineralization of electrospun collagen scaffolds for bone tissue engineering, Biomaterials 104 (2016) 323–338, https://doi.org/10.1016/j.biomaterials.2016.07.007.
[108] H.W. Kim, J.H. Song, H.E. Kim, Nanofiber generation of gelatin-hydroxyapatite biomimetics for guided tissue regeneration, Adv. Funct. Mater. 15 (2005) 1988–1994, https://doi.org/10.1002/adfm.200500116.
[109] Z. Xia, X. Yu, X. Jiang, H.D. Brody, D.W. Rowe, M. Wei, Fabrication and characterization of biomimetic collagen–apatite scaffolds with tunable structures for bone tissue engineering, Acta Biomater. 9 (2013) 7308–7319, https://doi.org/10.1016/j.actbio.2013.03.038.
[110] K. Yamauchi, T. Goda, N. Takeuchi, H. Einaga, T. Tanabe, Preparation of collagen/calcium phosphate multilayer sheet using enzymatic mineralization, Biomaterials 25 (2004) 5481–5489, https://doi.org/10.1016/j.biomaterials.2003.12.057.
[111] P.D. Dalton, T.B.F. Woodfield, V. Mironov, J. Groll, Advances in hybrid fabrication toward hierarchical tissue constructs, Adv. Sci. 7 (2020), 1902953, https://doi.org/10.1002/advs.201902953.
[112] Q.L. Loh, C. Choong, Three-dimensional scaffolds for tissue engineering applications: role of porosity and pore size, Tissue Eng. B Rev. 19 (2013) 485–502, https://doi.org/10.1089/ten.TEB.2012.0437.
[113] S. Bose, S. Vahabzadeh, A. Bandyopadhyay, Bone tissue engineering using 3D printing, Mater. Today 16 (2013) 496–504, https://doi.org/10.1016/j.mattod.2013.11.017.
[114] B. Grigoryan, S.J. Paulsen, D.C. Corbett, D.W. Sazer, C.L. Fortin, A.J. Zaita, P. T. Greenfield, N.J. Calafat, J.P. Gounley, A.H. Ta, F. Johansson, A. Randles, J. E. Rosenkrantz, J.D. Louis-Rosenberg, P.A. Galie, K.R. Stevens, J.S. Miller, Multivascular networks and functional intravascular topologies within biocompatible hydrogels, Science 364 (2019) 458–464, https://doi.org/10.1126/science.aav9750.
[115] F. Gao, Z.Y. Xu, Q.F. Liang, H.F. Li, L.Q. Peng, M.M. Wu, X.L. Zhao, X. Cui, C. S. Ruan, W.G. Liu, Osteochondral regeneration with 3D-printed biodegradable high-strength supramolecular polymer reinforced-gelatin hydrogel scaffolds, Adv. Sci. 6 (2019), 1900867, https://doi.org/10.1002/advs.201900867.
[116] Z.F. Lin, M.M. Wu, H.M. He, Q.F. Liang, C.S. Hu, Z.W. Zeng, D.L. Cheng, G. C. Wang, D.F. Chen, H.B. Pan, C.S. Ruan, 3D printing of mechanically stable calcium-free alginate-based scaffolds with tunable surface charge to enable cell adhesion and facile biofunctionalization, Adv. Funct. Mater. 29 (2019), 1808439, https://doi.org/10.1002/adfm.201808439.
[117] F. Gao, Z.Y. Xu, Q.F. Liang, B. Liu, H.F. Li, Y.H. Wu, Y.Y. Zhang, Z.F. Lin, M. M. Wu, C.S. Ruan, W.G. Liu, Direct 3D printing of high strength biohybrid gradient hydrogel scaffolds for efficient repair of osteochondral defect, Adv. Funct. Mater. 28 (2018), 1706644, https://doi.org/10.1002/adfm.201706644.
[118] Y.F. Ma, N. Hu, J. Liu, X.Y. Zhai, M.M. Wu, C.S. Hu, L. Li, Y.X. Lai, H.B. Pan, W. W. Lu, X.Z. Zhang, Y.F. Luo, C.S. Ruan, Three-dimensional printing of biodegradable piperazine-based polyurethane-urea scaffolds with enhanced osteogenesis for bone regeneration, ACS Appl. Mater. Interfaces 11 (2019) 9415–9424, https://doi.org/10.1021/acsami.8b20323.
[119] S. Ishack, A. Mediero, T. Wilder, J.L. Ricci, B.N. Cronstein, Bone regeneration in critical bone defects using three-dimensionally printed beta-tricalcium phosphate/hydroxyapatite scaffolds is enhanced by coating scaffolds with either dipyridamole or BMP-2, J. Biomed. Mater. Res. B 105 (2017) 366–375, https://doi.org/10.1002/jbm.b.33561.
[120] B. Charbonnier, M. Manassero, M. Bourguignon, A. Decambron, H. El-Hafci, C. Morin, D. Leon, M. Bensidoum, S. Corsia, H. Petite, D. Marchat, E. Potier, Custom-made macroporous bioceramic implants based on triply-periodic minimal surfaces for bone defects in load-bearing sites, Acta Biomater. 109 (2020) 254–266, https://doi.org/10.1016/j.actbio.2020.03.016.
[121] F. Fahimipour, E. Dashtimoghadam, M. Rasoulianboroujeni, M. Yazdimamaghani, K. Khoshroo, M. Tahriri, A. Yadegari, J.A. Gonzalez, D. Vashaee, D.C. Lobner, T. S. Jafarzadeh Kashi, L. Tayebi, Collagenous matrix supported by a 3D-printed scaffold for osteogenic differentiation of dental pulp cells, Dent. Mater. 34 (2018) 209–220, https://doi.org/10.1016/j.dental.2017.10.001.
[122] A. Lee, A.R. Hudson, D.J. Shiwarski, J.W. Tashman, T.J. Hinton, S. Yerneni, J. M. Bliley, P.G. Campbell, A.W. Feinberg, 3D bioprinting of collagen to rebuild components of the human heart, Science 365 (2019) 482–487, https://doi.org/10.1126/science.aav9051.
[123] S.V. Murphy, A. Atala, 3D bioprinting of tissues and organs, Nat. Biotechnol. 32 (2014) 773–785, https://doi.org/10.1038/nbt.2958.
[124] H.W. Kang, S.J. Lee, I.K. Ko, C. Kengla, J.J. Yoo, A. Atala, A 3D bioprinting system to produce human-scale tissue constructs with structural integrity, Nat. Biotechnol. 34 (2016) 312–319, https://doi.org/10.1038/nbt.3413.
[125] D.B. Kolesky, K.A. Homan, M.A. Skylar-Scott, J.A. Lewis, Three-dimensional bioprinting of thick vascularized tissues, Proc. Natl. Acad. Sci. U.S.A. 113 (2016) 3179–3184, https://doi.org/10.1073/pnas.1521342113.
[126] X. Ma, X. Qu, W. Zhu, Y.S. Li, S. Yuan, H. Zhang, J. Liu, P. Wang, C.S. Lai, F. Zanella, G.S. Feng, F. Sheikh, S. Chien, S. Chen, Deterministically patterned biomimetic human iPSC-derived hepatic model via rapid 3D bioprinting, Proc. Natl. Acad. Sci. U. S. A. 113 (2016) 2206–2211, https://doi.org/10.1073/pnas.1524510113.
[127] K.F. Lin, S. He, Y. Song, C.M. Wang, Y. Gao, J.Q. Li, P. Tang, Z. Wang, L. Bi, G. X. Pei, Low-temperature additive manufacturing of biomimic three-dimensional hydroxyapatite/collagen scaffolds for bone regeneration, ACS Appl. Mater. Interfaces 8 (2016) 6905–6916, https://doi.org/10.1021/acsami.6b00815.
[128] J.A. Inzana, D. Olvera, S.M. Fuller, J.P. Kelly, O.A. Graeve, E.M. Schwarz, S. L. Kates, H.A. Awad, 3D printing of composite calcium phosphate and collagen scaffolds for bone regeneration, Biomaterials 35 (2014) 4026–4034, https://doi.org/10.1016/j.biomaterials.2014.01.064.
[129] Q. Li, X.X. Lei, X.F. Wang, Z.G. Cai, P.J. Lyu, G.F. Zhang, Hydroxyapatite/collagen three-dimensional printed scaffolds and their osteogenic effects on human bone marrow-derived mesenchymal stem cells, Tissue Eng. 25 (2019) 1261–1271, https://doi.org/10.1089/ten.tea.2018.0201.
[130] W.J. Kim, H.-S. Yun, G.H. Kim, An innovative cell-laden α-TCP/collagen scaffold fabricated using a two-step printing process for potential application in regenerating hard tissues, Sci. Rep. 7 (2017), https://doi.org/10.1038/s41598-017-03455-9.
[131] R. Langer, J.P. Vacanti, Tissue engineering, Science 260 (1993) 920–926, https://doi.org/10.1126/science.8493529.
[132] K.J. Burg, S. Porter, J.F. Kellam, Biomaterial developments for bone tissue engineering, Biomaterials 21 (2000) 2347–2359, https://doi.org/10.1016/s0142-9612(00)00102-2.
[133] O.A. Tertuliano, J.R. Greer, The nanocomposite nature of bone drives its strength and damage resistance, Nat. Mater. 15 (2016) 1195–1202, https://doi.org/10.1038/nmat4719.
[134] M.A. Meyers, J. McKittrick, P.Y. Chen, Structural biological materials: critical mechanics-materials connections, Science 339 (2013) 773–779, https://doi.org/10.1126/science.1220854.
[135] T.D. Stocco, N.J. Bassous, S. Zhao, A.E.C. Granato, T.J. Webster, A.O. Lobo, Nanofibrous scaffolds for biomedical applications, Nanoscale 10 (2018) 12228–12255, https://doi.org/10.1039/c8nr02002g.
[136] S. Khosla, J.J. Westendorf, M.J. Oursler, Building bone to reverse osteoporosis and repair fractures, J. Clin. Invest. 118 (2008) 421–428, https://doi.org/10.1172/JCI33612.
[137] E.F. Eriksen, G.Z. Eghbali-Fatourechi, S. Khosla, Remodeling and vascular spaces in bone, J. Bone Miner. Res. 22 (2007) 1–6, https://doi.org/10.1359/jbmr.060910.
[138] J.P. Rys, D.A. Monteiro, T. Alliston, Mechanobiology of TGFbeta signaling in the skeleton, Matrix Biol. 52–54 (2016) 413–425, https://doi.org/10.1016/j.matbio.2016.02.002.
[139] E. Canalis, D.J. Adams, A. Boskey, K. Parker, L. Kranz, S. Zanotti, Notch signaling in osteocytes differentially regulates cancellous and cortical bone remodeling, J. Biol. Chem. 288 (2013) 25614–25625, https://doi.org/10.1074/jbc.M113.470492.
[140] M.G. Haugh, T.J. Vaughan, L.M. McNamara, The role of integrin alpha(V)beta(3) in osteocyte mechanotransduction, J Mech Behav Biomed Mater 42 (2015) 67–75, https://doi.org/10.1016/j.jmbbm.2014.11.001.
[141] B. Huo, X.L. Lu, K.D. Costa, Q. Xu, X.E. Guo, An ATP-dependent mechanism mediates intercellular calcium signaling in bone cell network under single cell nanoindentation, Cell Calcium 47 (2010) 234–241, https://doi.org/10.1016/j.ceca.2009.12.005.
[142] J. Li, E. Rose, D. Frances, Y. Sun, L. You, Effect of oscillating fluid flow stimulation on osteocyte mRNA expression, J. Biomech. 45 (2012) 247–251, https://doi.org/10.1016/j.jbiomech.2011.10.037.
[143] S.P. Fritton, S. Weinbaum, Fluid and solute transport in bone: flow-induced mechanotransduction, Annu. Rev. Fluid Mech. 41 (2009) 347–374, https://doi.org/10.1146/annurev.fluid.010908.165136.
[144] M.D. Aisha, M.N. Nor-Ashikin, A.B. Sharaniza, H. Nawawi, G.R. Froemming, Orbital fluid shear stress promotes osteoblast metabolism, proliferation and alkaline phosphates activity in vitro, Exp. Cell Res. 337 (2015) 87–93, https://doi.org/10.1016/j.yexcr.2015.07.002.
[145] X. Niu, L. Wang, F. Tian, L. Wang, P. Li, Q. Feng, Y. Fan, Shear-mediated crystallization from amorphous calcium phosphate to bone apatite, J Mech Behav Biomed Mater 54 (2016) 131–140, https://doi.org/10.1016/j.jmbbm.2015.09.024.
[146] N. Saeidi, On the Control of Collagen Fibril Organization and Morphology, Mechanical Engineering Dissertations, 2009. http://hdl.handle.net/2047/d20000060.
[147] X.F. Niu, R. Fan, X.L. Guo, T.M. Du, Z. Yang, Q.L. Feng, Y.B. Fan, Shear-mediated orientational mineralization of bone apatite on collagen fibrils, J. Mater. Chem. B 5 (2017) 9141–9147, https://doi.org/10.1039/c7tb02223a.
[148] T. Du, X. Niu, S. Hou, M. Xu, Z. Li, P. Li, Y. Fan, Highly aligned hierarchical intrafibrillar mineralization of collagen induced by periodic fluid shear stress, J. Mater. Chem. B 8 (2020) 2562–2572, https://doi.org/10.1039/c9tb02643f.
[149] Y. Zhang, M.Q. Zhang, Three-dimensional macroporous calcium phosphate bioceramics with nested chitosan sponges for load-bearing bone implants, J. Biomed. Mater. Res. 61 (2002) 1–8, https://doi.org/10.1002/jbm.10176.
[150] F.J. O'Brien, B.A. Harley, I.V. Yannas, L.J. Gibson, The effect of pore size on cell adhesion in collagen-GAG scaffolds, Biomaterials 26 (2005) 433–441, https://doi.org/10.1016/j.biomaterials.2004.02.052.
[151] S.H. Hsu, H.J. Yen, C.S. Tseng, C.S. Cheng, C.L. Tsai, Evaluation of the growth of chondrocytes and osteoblasts seeded into precision scaffolds fabricated by fused deposition manufacturing, J. Biomed. Mater. Res. B 80 (2007) 519–527, https://doi.org/10.1002/jbm.b.30626.

[152] I.L. Ardelean, D. Gudovan, D. Ficai, A. Ficai, E. Andronescu, M.G. Albu-Kaya, P. Neacsu, R.N. Ion, A. Cimpean, V. Mitran, Collagen/hydroxyapatite bone grafts manufactured by homogeneous/heterogeneous 3D printing, Mater. Lett. 231 (2018) 179–182, https://doi.org/10.1016/j.matlet.2018.08.042.
[153] G.M. Cunniffe, G.R. Dickson, S. Partap, K.T. Stanton, F.J. O'Brien, Development and characterisation of a collagen nano-hydroxyapatite composite scaffold for bone tissue engineering, J. Mater. Sci. Mater. Med. 21 (2010) 2293–2298, https://doi.org/10.1007/s10856-009-3964-1.
[154] C.K.F. Chan, G.S. Gulati, R. Sinha, J.V. Tompkins, M. Lopez, A.C. Carter, R. C. Ransom, A. Reinisch, T. Wearda, M. Murphy, R.E. Brewer, L.S. Koepke, O. Marecic, A. Manjunath, E.Y. Seo, T. Leavitt, W.J. Lu, A. Nguyen, S.D. Conley, A. Salhotra, T.H. Ambrosi, M.R. Borrelli, T. Siebel, K. Chan, K. Schallmoser, J. Seita, D. Sahoo, H. Goodnough, J. Bishop, M. Gardner, R. Majeti, D.C. Wan, S. Goodman, I.L. Weissman, H.Y. Chang, M.T. Longaker, Identification of the human skeletal stem cell, Cell 175 (2018) 43–56, https://doi.org/10.1016/j.cell.2018.07.029.
[155] L. Yu, Y. Yang, B. Zhang, X. Bai, Q. Fei, L. Zhang, Rapid human-derived iPSC osteogenesis combined with three-dimensionally printed Ti6Al4V scaffolds for the repair of bone defects, J. Cell. Physiol. (2020) 1–10, https://doi.org/10.1002/jcp.29788.
[156] C. Fu, D. Luo, M. Yu, N. Jiang, D. Liu, D. He, Y. Fu, T. Zhang, Y. Qiao, Y. Zhou, Y. Liu, Embryonic-like mineralized extracellular matrix/stem cell microspheroids as a bone graft substitute, Adv Healthc Mater 7 (2018), e1800705, https://doi.org/10.1002/adhm.201800705.
[157] K.M. Woo, J.H. Jun, V.J. Chen, J. Seo, J.H. Baek, H.M. Ryoo, G.S. Kim, M. J. Somerman, P.X. Ma, Nano-fibrous scaffolding promotes osteoblast differentiation and biomineralization, Biomaterials 28 (2007) 335–343, https://doi.org/10.1016/j.biomaterials.2006.06.013.
[158] K.M. Woo, V.J. Chen, P.X. Ma, Nano-fibrous scaffolding architecture selectively enhances protein adsorption contributing to cell attachment, J. Biomed. Mater. Res. 67 (2003) 531–537, https://doi.org/10.1002/jbm.a.10098.
[159] M. Dang, L. Saunders, X. Niu, Y. Fan, P.X. Ma, Biomimetic delivery of signals for bone tissue engineering, Bone Res 6 (2018) 25, https://doi.org/10.1038/s41413-018-0025-8.
[160] M.O. Montjovent, N. Burri, S. Mark, E. Federici, C. Scaletta, P.Y. Zambelli, P. Hohlfeld, P.F. Leyvraz, L.L. Applegate, D.P. Pioletti, Fetal bone cells for tissue engineering, Bone 35 (2004) 1323–1333, https://doi.org/10.1016/j.bone.2004.07.001.
[161] R. Quarto, M. Mastrogiacomo, R. Cancedda, S.M. Kutepov, V. Mukhachev, A. Lavroukov, E. Kon, M. Marcacci, Repair of large bone defects with the use of autologous bone marrow stromal cells, N. Engl. J. Med. 344 (2001) 385–386, https://doi.org/10.1056/nejm200102013440516.
[162] S. Sethe, A. Scutt, A. Stolzing, Aging of mesenchymal stem cells, Ageing Res. Rev. 5 (2006) 91–116, https://doi.org/10.1016/j.arr.2005.10.001.
[163] J. Hu, K. Feng, X. Liu, P.X. Ma, Chondrogenic and osteogenic differentiations of human bone marrow-derived mesenchymal stem cells on a nanofibrous scaffold with designed pore network, Biomaterials 30 (2009) 5061–5067, https://doi.org/10.1016/j.biomaterials.2009.06.013.
[164] X. Xin, M. Hussain, J.J. Mao, Continuing differentiation of human mesenchymal stem cells and induced chondrogenic and osteogenic lineages in electrospun PLGA nanofiber scaffold, Biomaterials 28 (2007) 316–325, https://doi.org/10.1016/j.biomaterials.2006.08.042.
[165] M.J. Evans, M.H. Kaufman, Establishment in culture of pluripotential cells from mouse embryos, Nature 292 (1981) 154–156, https://doi.org/10.1038/292154a0.
[166] E.K.A. Nur, I. Ahmed, J. Kamal, M. Schindler, S. Meiners, Three-dimensional nanofibrillar surfaces promote self-renewal in mouse embryonic stem cells, Stem Cell. 24 (2006) 426–433, https://doi.org/10.1634/stemcells.2005-0170.
[167] X. Zeng, M.S. Rao, Human embryonic stem cells: long term stability, absence of senescence and a potential cell source for neural replacement, Neuroscience 145 (2007) 1348–1358, https://doi.org/10.1016/j.neuroscience.2006.09.017.
[168] K. Takahashi, S. Yamanaka, Induction of pluripotent stem cells from mouse embryonic and adult fibroblast cultures by defined factors, Cell 126 (2006) 663–676, https://doi.org/10.1016/j.cell.2006.07.024.
[169] J. Yu, M.A. Vodyanik, K. Smuga-Otto, J. Antosiewicz-Bourget, J.L. Frane, S. Tian, J. Nie, G.A. Jonsdottir, V. Ruotti, R. Stewart, Slukvin II, J.A. Thomson, Induced pluripotent stem cell lines derived from human somatic cells, Science 318 (2007) 1917–1920, https://doi.org/10.1126/science.1151526.
[170] P. De Coppi, G. Bartsch Jr., M.M. Siddiqui, T. Xu, C.C. Santos, L. Perin, G. Mostoslavsky, A.C. Serre, E.Y. Snyder, J.J. Yoo, M.E. Furth, S. Soker, A. Atala, Isolation of amniotic stem cell lines with potential for therapy, Nat. Biotechnol. 25 (2007) 100–106, https://doi.org/10.1038/nbt1274.
[171] D. Nguyen, D.A. Hagg, A. Forsman, J. Ekholm, P. Nimkingratana, C. Brantsing, T. Kalogeropoulos, S. Zaunz, S. Concaro, M. Brittberg, A. Lindahl, P. Gatenholm, A. Enejder, S. Simonsson, Cartilage tissue engineering by the 3D bioprinting of iPS cells in a nanocellulose/alginate bioink, Sci. Rep. 7 (2017) 658, https://doi.org/10.1038/s41598-017-00690-y.
[172] C.L. Kao, L.K. Tai, S.H. Chiou, Y.J. Chen, K.H. Lee, S.J. Chou, Y.L. Chang, C. M. Chang, S.J. Chen, H.H. Ku, H.Y. Li, Resveratrol promotes osteogenic differentiation and protects against dexamethasone damage in murine induced pluripotent stem cells, Stem Cell. Dev. 19 (2010) 247–258, https://doi.org/10.1089/scd.2009.0186.
[173] G. Bilousova, D.H. Jun, K.B. King, S. De Langhe, W.S. Chick, E.C. Torchia, K. S. Chow, D.J. Klemm, D.R. Roop, S.M. Majka, Osteoblasts derived from induced pluripotent stem cells form calcified structures in scaffolds both in vitro and in vivo, Stem Cell. 29 (2011) 206–216, https://doi.org/10.1002/stem.566.
[174] X. Xian, R. Moraghebi, H. Lofvall, A. Fasth, K. Henriksen, J. Richter, N.B. Woods, I. Moscatelli, Generation of gene-corrected functional osteoclasts from osteopetrotic induced pluripotent stem cells, Stem Cell Res. Ther. 11 (2020) 179, https://doi.org/10.1186/s13287-020-01701-y.
[175] A. Ho-Shui-Ling, J. Bolander, L.E. Rustom, A.W. Johnson, F.P. Luyten, C. Picart, Bone regeneration strategies: engineered scaffolds, bioactive molecules and stem cells current stage and future perspectives, Biomaterials 180 (2018) 143–162, https://doi.org/10.1016/j.biomaterials.2018.07.017.
[176] H. Hosseinkhani, M. Hosseinkhani, A. Khademhosseini, H. Kobayashi, Bone regeneration through controlled release of bone morphogenetic protein-2 from 3-D tissue engineered nano-scaffold, J. Contr. Release 117 (2007) 380–386, https://doi.org/10.1016/j.jconrel.2006.11.018.
[177] K.C. Nune, A. Kumar, L.E. Murr, R.D. Misra, Interplay between self-assembled structure of bone morphogenetic protein-2 (BMP-2) and osteoblast functions in three-dimensional titanium alloy scaffolds: stimulation of osteogenic activity, J. Biomed. Mater. Res. 104 (2016) 517–532, https://doi.org/10.1002/jbm.a.35592.
[178] Z.Y. Lin, Z.X. Duan, X.D. Guo, J.F. Li, H.W. Lu, Q.X. Zheng, D.P. Quan, S.H. Yang, Bone induction by biomimetic PLGA-(PEG-ASP)n copolymer loaded with a novel synthetic BMP-2-related peptide in vitro and in vivo, J. Contr. Release 144 (2010) 190–195, https://doi.org/10.1016/j.jconrel.2010.02.016.
[179] H. Wang, G. Wu, J. Zhang, K. Zhou, B. Yin, X. Su, G. Qiu, G. Yang, X. Zhang, G. Zhou, Z. Wu, Osteogenic effect of controlled released rhBMP-2 in 3D printed porous hydroxyapatite scaffold, Colloids Surf., B 141 (2016) 491–498, https://doi.org/10.1016/j.colsurfb.2016.02.007.
[180] J.S. Sun, F.H. Lin, Y.J. Wang, Y.C. Huang, S.C. Chueh, F.Y. Hsu, Collagen-hydroxyapatite/tricalcium phosphate microspheres as a delivery system for recombinant human transforming growth factor-beta 1, Artif. Organs 27 (2003) 605–612, https://doi.org/10.1046/j.1525-1594.2003.07169.x.
[181] A. Mishra, P. Tummala, A. King, B. Lee, M. Kraus, V. Tse, C.R. Jacobs, Buffered platelet-rich plasma enhances mesenchymal stem cell proliferation and chondrogenic differentiation, Tissue Eng. Part C 15 (2009) 431–435, https://doi.org/10.1089/ten.tec.2008.0534.
[182] W. Kim, C.H. Jang, G. Kim, Optimally designed collagen/polycaprolactone biocomposites supplemented with controlled release of HA/TCP/rhBMP-2 and HA/TCP/PRP for hard tissue regeneration, Mater. Sci. Eng. C 78 (2017) 763–772, https://doi.org/10.1016/j.msec.2017.04.144.
[183] H. Komaki, T. Tanaka, M. Chazono, T. Kikuchi, Repair of segmental bone defects in rabbit tibiae using a complex of β-tricalcium phosphate, type I collagen, and fibroblast growth factor-2, Biomaterials 27 (2006) 5118–5126, https://doi.org/10.1016/j.biomaterials.2006.05.031.
[184] W. Saito, K. Uchida, M. Ueno, O. Matsushita, G. Inoue, N. Nishi, T. Ogura, S. Hattori, H. Fujimaki, K. Tanaka, M. Takaso, Acceleration of bone formation during fracture healing by injectable collagen powder and human basic fibroblast growth factor containing a collagen-binding domain fromClostridium histolyticumcollagenase, J. Biomed. Mater. Res. 102 (2014) 3049–3055, https://doi.org/10.1002/jbm.a.34974.
[185] C.S. Young, G. Bradica, C.E. Hart, A. Karunanidhi, R.M. Street, L. Schutte, J. O. Hollinger, J.-H. Jang, Preclinical toxicology studies of recombinant human platelet-derived growth factor-BB either alone or in combination with beta-tricalcium phosphate and type I collagen, J. Tissue Eng. 1 (2010), 246215. http://doi.org/10.4061/2010/246215.
[186] J.O. Hollinger, A.O. Onikepe, J. MacKrell, T. Einhorn, G. Bradica, S. Lynch, C. E. Hart, Accelerated fracture healing in the geriatric, osteoporotic rat with recombinant human platelet-derived growth factor-BB and an injectable beta-tricalcium phosphate/collagen matrix, J. Orthop. Res. 26 (2008) 83–90, https://doi.org/10.1002/jor.20453.
[187] M.B. Sporn, G.J. Todaro, Autocrine secretion and malignant transformation of cells, N. Engl. J. Med. 303 (1980) 878–880, https://doi.org/10.1056/nejm198010093031511.
[188] L.A. Fortier, J.U. Barker, E.J. Strauss, T.M. McCarrel, B.J. Cole, The role of growth factors in cartilage repair, Clin. Orthop. Relat. Res. 469 (2011) 2706–2715, https://doi.org/10.1007/s11999-011-1857-3.
[189] J.H. Song, H.E. Kim, H.W. Kim, Electrospun fibrous web of collagen-apatite precipitated nanocomposite for bone regeneration, J. Mater. Sci. Mater. Med. 19 (2008) 2925–2932, https://doi.org/10.1007/s10856-008-3420-7.
[190] H. Zheng, Y. Bai, M.S. Shih, C. Hoffmann, F. Peters, C. Waldner, W.D. Hubner, Effect of a beta-TCP collagen composite bone substitute on healing of drilled bone voids in the distal femoral condyle of rabbits, J. Biomed. Mater. Res. B 102 (2014) 376–383, https://doi.org/10.1002/jbm.b.33016.
[191] D. Zhang, X. Wu, J. Chen, K. Lin, The development of collagen based composite scaffolds for bone regeneration, Bioact Mater 3 (2018) 129–138, https://doi.org/10.1016/j.bioactmat.2017.08.004.
[192] M. Sartori, S. Pagani, A. Ferrari, V. Costa, V. Carina, E. Figallo, M.C. Maltarello, L. Martini, M. Fini, G. Giavaresi, A new bi-layered scaffold for osteochondral tissue regeneration: in vitro and in vivo preclinical investigations, Mater. Sci. Eng. C 70 (2017) 101–111, https://doi.org/10.1016/j.msec.2016.08.027.
[193] S. Minardi, B. Corradetti, F. Taraballi, M. Sandri, J. Van Eps, F.J. Cabrera, B. K. Weiner, A. Tampieri, E. Tasciotti, Evaluation of the osteoinductive potential of a bio-inspired scaffold mimicking the osteogenic niche for bone augmentation, Biomaterials 62 (2015) 128–137, https://doi.org/10.1016/j.biomaterials.2015.05.011.
[194] G. Calabrese, R. Giuffrida, S. Forte, L. Salvatorelli, C. Fabbi, E. Figallo, M. Gulisano, R. Parenti, G. Magro, C. Colarossi, L. Memeo, R. Gulino, Bone augmentation after ectopic implantation of a cell-free collagen-hydroxyapatite

scaffold in the mouse, Sci. Rep. 6 (2016), 36399, https://doi.org/10.1038/srep36399.
[195] W. Yu, T.W. Sun, C. Qi, Z. Ding, H. Zhao, S. Zhao, Z. Shi, Y.J. Zhu, D. Chen, Y. He, Evaluation of zinc-doped mesoporous hydroxyapatite microspheres for the construction of a novel biomimetic scaffold optimized for bone augmentation, Int. J. Nanomed. 12 (2017) 2293–2306. http://doi.org/10.2147/IJN.S126505.
[196] S. Liao, M. Ngiam, F. Watari, S. Ramakrishna, C.K. Chan, Systematic fabrication of nano-carbonated hydroxyapatite/collagen composites for biomimetic bone grafts, Bioinspiration Biomimetics 2 (2007) 37–41, https://doi.org/10.1088/1748-3182/2/3/001.
[197] U. Lindert, W.A. Cabral, S. Ausavarat, S. Tongkobpetch, K. Ludin, A.M. Barnes, P. Yeetong, M. Weis, B. Krabichler, C. Srichomthong, E.N. Makareeva, A. R. Janecke, S. Leikin, B. Rothlisberger, M. Rohrbach, I. Kennerknecht, D.R. Eyre, K. Suphapeetiporn, C. Giunta, J.C. Marini, V. Shotelersuk, MBTPS2 mutations cause defective regulated intramembrane proteolysis in X-linked osteogenesis imperfecta, Nat. Commun. 7 (2016), 11920, https://doi.org/10.1038/ncomms11920.
[198] E. Banks, S. Nakajima, L. Shapiro, O. Tilevitz, Alonzo, R. Chianelli, Fibrous apatite grown on modified collagen, Science 198 (1977) 1164–1166, https://doi.org/10.1126/science.929194.
[199] M. Kikuchi, H.N. Matsumoto, T. Yamada, Y. Koyama, K. Takakuda, J. Tanaka, Glutaraldehyde cross-linked hydroxyapatite/collagen self-organized nanocomposites, Biomaterials 25 (2004) 63–69, https://doi.org/10.1016/s0142-9612(03)00472-1.
[200] T.M. Du, X.F. Niu, Z.W. Li, P. Li, Q.L. Feng, Y.B. Fan, Crosslinking induces high mineralization of apatite minerals on collagen fibers, Int. J. Biol. Macromol. 113 (2018) 450–457, https://doi.org/10.1016/j.ijbiomac.2018.02.136.
[201] F. Gao, C.S. Ruan, W.G. Liu, High-strength hydrogel-based bioinks, Mat Chem Front 3 (2019) 1736–1746, https://doi.org/10.1039/c9qm00373h.
[202] X. Ge, Z. Xia, S. Guo, Recent advances on black phosphorus for biomedicine and biosensing, Adv. Funct. Mater. 29 (2019), 1900318, https://doi.org/10.1002/adfm.201900318.
[203] W. Chen, J. Ouyang, X. Yi, Y. Xu, C. Niu, W. Zhang, L. Wang, J. Sheng, L. Deng, Y. N. Liu, S. Guo, Black phosphorus nanosheets as a neuroprotective nanomedicine for neurodegenerative disorder therapy, Adv. Mater. 30 (2018), 1703458, https://doi.org/10.1002/adma.201703458.
[204] S.T. Han, L. Hu, X. Wang, Y. Zhou, Y.J. Zeng, S. Ruan, C. Pan, Z. Peng, Black phosphorus quantum dots with tunable memory properties and multilevel resistive switching characteristics, Adv. Sci. 4 (2017), 1600435, https://doi.org/10.1002/advs.201600435.
[205] J. Liu, P. Du, T. Liu, B.J. Cordova Wong, W. Wang, H. Ju, J. Lei, A black phosphorus/manganese dioxide nanoplatform: oxygen self-supply monitoring, photodynamic therapy enhancement and feedback, Biomaterials 192 (2019) 179–188, https://doi.org/10.1016/j.biomaterials.2018.10.018.
[206] L. Cheng, Z. Cai, J. Zhao, F. Wang, M. Lu, L. Deng, W. Cui, Black phosphorus-based 2D materials for bone therapy, Bioact Mater 5 (2020) 1026–1043, https://doi.org/10.1016/j.bioactmat.2020.06.007.
[207] Q. Zhou, Q. Chen, Y. Tong, J. Wang, Light-induced ambient degradation of few-layer black phosphorus: mechanism and protection, Angew Chem. Int. Ed. Engl. 55 (2016) 11437–11441, https://doi.org/10.1002/anie.201605168.
[208] Y. Zhou, M. Zhang, Z. Guo, L. Miao, S.-T. Han, Z. Wang, X. Zhang, H. Zhang, Z. Peng, Recent advances in black phosphorus-based photonics, electronics, sensors and energy devices, Mater Horiz 4 (2017) 997–1019, https://doi.org/10.1039/c7mh00543a.
[209] J. Shao, C. Ruan, H. Xie, P.K. Chu, X.F. Yu, Photochemical activity of black phosphorus for near-infrared light controlled in situ biomineralization, Adv. Sci. (2020), 2000439, https://doi.org/10.1002/advs.202000439.
[210] T. Nishikawa, K. Masuno, K. Tominaga, Y. Koyama, T. Yamada, K. Takakuda, M. Kikuchi, J. Tanaka, A. Tanaka, Bone repair analysis in a novel biodegradable hydroxyapatite/collagen composite implanted in bone, Implant Dent. 14 (2005) 252–260, https://doi.org/10.1097/01.id.0000173628.00705.d0.